REPORT No. 335

AERODYNAMIC THEORY AND TEST OF STRUT FORMS—II

By R. H. SMITH

Aerodynamical Laboratory
Bureau of Construction and Repair
U. S. Navy

FOREWORD

The author wishes to express his sincere thanks to Dr. A. F. Zahm for his valuable advice and encouragement during the time this work was being accomplished and for his interest in the progress of the experimental results; also to the Bureau of Aeronautics and to the Bureau of Construction and Repair, United States Navy, whose interest and laboratory equipment in Washington, where the work was done, have made these studies possible.

722

REPORT No. 335

AERODYNAMIC THEORY AND TEST OF STRUT FORMS—PART II[1]

By R. H. SMITH

SUMMARY

This report, submitted to the National Advisory Committee for Aeronautics for publication, presents the second of two studies under the same title. In this part five theoretical struts are developed from distributed sources and sinks and constructed for pressure and resistance tests in a wind tunnel. The surface pressures for symmetrical inviscid flow are computed for each strut from theory and compared with those found by experiment. The theoretical and experimental pressures are found to agree quantitatively near the bow, only qualitatively over the suction range, the experimental suctions being uniformly a little low, and not at all near the stern.

This study is the strut sequel to Fuhrmann's research on airship forms, the one being a study in two dimensions, the other in three. A comparison of results indicates that the agreement between theory and experiment is somewhat better for bodies of revolution than for cylinders when both are shaped for slight resistance. The consistent deficiency of the experimental suctions which is found in the case of struts was not found in the case of airships, for which the experimental suctions were sometimes above sometimes below their theoretical values.

Along with these five theoretical struts were made three empirical struts of high repute, the British strut given in Reports and Memoranda Number 183, the German strut Number 53, and the United States Navy Number 2, and all eight tested for total resistance. Of the five theoretical struts, Number I excels as a fairing, Number V as a strut. Number V and the United States Navy Number 2 have about equal merit as struts, with the German Number 53 a close second and the British a poor third, the relative merits being 100, 103, and 112, respectively, of Reynolds Number 12×10^4.

---

[1] This part was submitted in May, 1929, to the Johns Hopkins University as a doctor's dissertation. Part I was reported in Reference 10.

AERODYNAMIC THEORY AND TEST OF STRUT FORMS—PART II

By R. H. SMITH

INTRODUCTION[1]

In Part I of this study we were concerned, among other things, with the inverse problem of finding a source-sink distribution whose flow boundary in a uniform stream was the surface of a given empirical strut of high service merit, and then of finding the theoretical pressure everywhere on the strut surface. We will now consider, in Part II, the direct problem of finding the flow boundaries, in a uniform stream, of a few balanced combinations of sources and sinks whose types of distribution are predetermined, and then of finding, as before, the theoretical pressure on the boundary surfaces. Strut models whose surfaces coincide with these flow boundaries will then be made and tested in a wind tunnel for surface pressure and total resistance.

The direct-problem study is analogous to that made by Fuhrmann on a series of surfaces of revolution resembling airships. (Ref. 1.) Part II may therefore be considered as the strut sequel to Fuhrmann's investigation, the one being a study in two dimensions, the other in three.[2] Before beginning the study, however, it may be well to consider, very briefly, a portion of the underlying mathematics leading to the basic equations of two-dimensional potential flow.

THE FUNDAMENTAL EQUATIONS

A general vector field, such as the distribution of velocity, V, throughout a moving mass of fluid, can always be resolved into two component fields, each present as if alone. One of these components, called the rotational field, arises from vortices and has curl but no divergence, the other, called the irrotational field, arises from sources and sinks and has divergence but no curl. The functional form of V for either component field is obviously fixed by the condition of absence of the other; that is, in the rotational field, V must be curl F, where F is a vector, in order to have no divergence, and in the irrotational field, V must be grad φ, where φ is a scalar, in order to have no curl. Accordingly the rotational component field has the equation

$$\text{curl } V = \text{curl curl } F \tag{1}$$

and the irrotational component field has the equation

$$\text{div } V = \text{div grad } \varphi \tag{2}$$

Vector fields whose rotational components are absent are always expressed in terms of scalar or potential fields as in equation (2) because of the great simplification of treatment which ensues.[3] When this substitution can be made—that is, when the field is irrotational—it is susceptible to manageable treatment even when the sources and sinks which produce it are quite complex.

The present study includes an investigation of the velocity and pressure in a uniform stream of perfect fluid flowing symmetrically past each of five Rankine struts. The velocity field is therefore produced entirely by sources and sinks; hence is irrotational and susceptible to analysis

---

[1] See the general introduction, Part I, Reference 10.

[2] Part II was suggested to me by Dr. A. F. Zahm as suitable for a thesis.

[3] It should be recalled that there are special circulatory fields which are irrotational and which are therefore expressible in terms of scalar fields. These fields are produced by line vortices which induce circumferential velocities inversely proportional to the radii.

by equation (2). If we assume the air to be incompressible,[4] and if we allow for the strength of the sources and sinks enclosed by the closed path of integration, equation (2) becomes.

$$\text{div } V = \text{div grad } \varphi = \Delta^2 \varphi = 0 \quad\text{------------------------------} \quad (3)$$

Equation (3) is invariant to coordinate axes. If we choose cylindrical coordinates for the purpose of deriving the basic equations for this study, and if we assume for V axial symmetry about, and uniformity along z, equation (3) becomes,

$$\Delta^2 \varphi = \frac{1}{\rho} \frac{\partial}{\partial \rho}\left(\rho \frac{\partial \varphi}{\partial \rho}\right) = 0 \quad\text{------------------------------} \quad (4)$$

Since one is concerned with φ at finite distances, equation (4) may be written

$$\rho \frac{\partial \varphi}{\partial \rho} = C \quad\text{------------------------------} \quad (5)$$

from which clearly—

$$\varphi = Cln\rho + A \quad\text{------------------------------} \quad (6)$$

In equation (6), $Cln\rho$ is the potential due to a line source whose strength per unit length is $2 \pi C$ [5] and A is an added potential of a flow with no divergence such as the potential of a uniform superimposed stream. If this uniform stream has the velocity U along x normal to the source then $A = Ux$, because at great distances where the velocity of the flow from the source vanishes, A satisfies the boundary condition,

$$V_x = \frac{\partial \varphi}{\partial x} = \frac{\partial A}{\partial x} = U$$

Equation (6) then becomes

$$\varphi = Cln\rho + Ux \quad\text{------------------------------} \quad (7)$$

Each term of equation (7), being a two-dimensional potential, must have a conjugate which satisfies the equation

$$\varphi + i\psi = f(z)$$

The conjugate to $Cln\rho$ is seen to be $C\theta$ upon decomposing

$$\varphi + i\psi = Cln \; z = Cln \; (\rho \; e^{i\theta})$$

into its real and imaginary parts, and the conjugate to Ux is clearly Uy upon decomposing,

$$\varphi + i\psi = Uz = U \; (x + iy).$$

Accordingly the velocity potential, φ, and the stream function, ψ, of the flow from a line source along z and of a superimposed uniform stream normal to z, are given by the two equations—

$$\varphi = Cln\rho + Ux \quad\text{------------------------------} \quad (8)$$
$$\psi = C\theta + Uy \quad\text{------------------------------} \quad (9)$$

THE RANKINE HALF STRUT

Preliminary to the treatment of the Rankine struts proper, a study of the half strut, which is produced by a line source normal to a uniform stream, will be made for two reasons; it will be useful in illustrating, in their simplest application, the analytics and the graphics which will be required in the strut development, and, secondly, it has considerable academic interest of its own.

---

[4] The correction to divergence due to adiabatic compression is negligibly small in air flowing past a strut under ordinary flight conditions. (Ref. 8.)

[5] The strength of a line source per unit length is $2 \pi \rho v_\rho$. From equation (5) $v_\rho = \frac{C}{\rho}$, hence the source strength per unit length is $2\pi C$.

THEORETICAL TREATMENT

Let the contour of the half strut, which is the boundary surface between the source flow and the uniform stream, be $a\ b\ c\ d$, and let the source be at 0, Figure 1. Choose any point p inside, on or outside the boundary surface, and let pp_0 be its ordinate. We wish to express the stream function at p. Since the stream function may be considered physically as a flux across a line, a choice will be made at the outset between the arc pq and the ordinate pp_0. Equation (9), of course, gives the flux across the arc, and mathematically this is the better choice. However, the equipotential diagram of flux across the ordinate (fig. 7) is more easily interpreted physically and has a symmetry lacking in the diagram of flux across the arc, due to a difference in those parts of the diagrams pertaining to the second quadrant of the field.[6] On the other hand the ordinate interpretation requires that the half strength, πC, of the source be deducted from the stream function, ψ, at all points of the field. The deduction is required when θ is greater than $\frac{\pi}{2}$ to convert ψ from a flux across the arc to a flux across the ordinate, and when less than $\frac{\pi}{2}$ to compensate for the additional flux from the source across pp_0 as compared to that across rr_0

(fig. 1) when a uniform stream is superimposed.[7] Hence the deduction, πC, while a simple constant mathematically, is two constants physically, each of which should be applied to different quadrants of the field, at different stages in the development and for different physical reasons.

FIGURE 1

Since even in the case of distributed sources both parts of the deduction are quite simple ones to compute, and since it seems best to clarify the interpretation of the diagrams, which have a certain value in themselves, the ordinate interpretation will be assumed and the deductions separated. This choice has also the important advantage of following the procedure of Fuhrmann.

Having made this choice we may write equation (9) in two parts corresponding to the two quadrants of the field,

$$\frac{\psi}{C} = -(\pi-\theta)+\frac{y}{a}, \quad x<0$$
$$\frac{\psi}{C} = \theta +\frac{y}{a}-\pi, \quad x>0$$
[8] \hfill (10)

where $a = \dfrac{C}{U}$.

The equation of the half strut, given by letting $\psi=0$ and $y=\rho\sin\theta$ in equation (10), is

$$\rho = a\frac{\pi-\theta}{\sin\theta} \hfill (11)$$

From equation (11), the bow, b, is at $x_0 = -a$. (Fig. 1.) Going aft, the boundary surface intercepts the y axis at $y_0 = \pm\frac{\pi}{2}a$ and approaches asymptotically the two planes $y = \pm\pi a$ Since the parameter a is clearly a measure of the dimensions of the half strut, a series of values of a will give a series of similar contours with the source line as their common focus.

---

[6] When the arc has second quadrant magnitude, θ for the arc diagram becomes $-(\pi-\theta)$ for the ordinate diagram, the minus sign indicating a right to left flux across the ordinate.

[7] Since both rp and bcp' (fig. 1) are streamlines, no fluid crosses either and the flux across rr_0 is equal to that across pp' or to that across pp_0 decreased by πC, the half strength of the source.

[8] Considered mathematically, equation (10) is simply equation (9) with the constant potential $-\pi C$ added in order that the body may have the equation $\psi=0$ and then written in two forms so that only acute angles enter, which avoids ambiguity in the sign of the trigonometric functions.
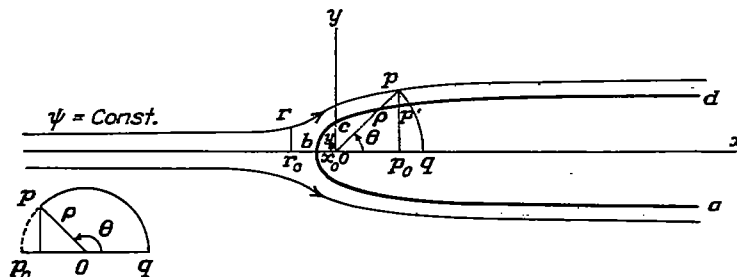
Upon partial differentiation, equation (10) gives, at each point of the field, the component velocities

$$V_x = \frac{\partial \psi}{\partial y} = C\frac{x}{\rho^2} + U$$

$$V_y = -\frac{\partial \psi}{\partial x} = C\frac{y}{\rho^2}$$

whose resultant squared is,

$$V^2 = \frac{C^2}{\rho^2}\left(1 + 2\frac{x}{a}\right) + U^2 \text{\textemdash\textemdash\textemdash\textemdash\textemdash\textemdash\textemdash\textemdash\textemdash\textemdash\textemdash\textemdash\textemdash\textemdash} \tag{12}$$

If one defines p_n as the full impact pressure of the stream and p as the superstream pressure, or as the pressure above or below that of the distant stream, then, for steady flow,

$$\frac{p}{p_n} = 1 - \left(\frac{V}{U}\right)^2 \text{\textemdash\textemdash\textemdash\textemdash\textemdash\textemdash\textemdash\textemdash\textemdash\textemdash\textemdash\textemdash} \tag{13}$$

or

$$\frac{p}{p_n} = -\left(\frac{a^2}{\rho^2} + 2\frac{a}{\rho}\cos\theta\right) \text{\textemdash\textemdash\textemdash\textemdash\textemdash\textemdash\textemdash\textemdash\textemdash\textemdash} \tag{14}$$

The curve of pressure $\frac{p}{p_n}$ versus the distance x aft the bow, plotted from equation (14) in Figure 5, shows that the pressure is a maximum at the nose, as usual, where it equals the full impact pressure of the uniform stream. Going aft, the pressure decreases rather sharply, passes through its zero value at $x = \frac{a}{2}$ and reaches a negative maximum from which it gradually subsides asymptotically to zero.

At any surface element of the half strut, the pressure exerts on the strut a drag, $p\,dy$ per unit length, whose integral over any zone or strip of the surface is the zonal pressural drag. (Ref. 2.)   If D is the zonal drag per unit length,

$$D = 2\int_{y_1}^{y_2} p\,dy,$$

or $$D = -2a\ p_n \int_{\theta_1}^{\theta_2} \frac{1}{\rho^2}(a + 2\rho\cos\theta)\ (\rho\cos\theta\ d\theta + \sin\theta\ d\rho) \text{\textemdash\textemdash\textemdash\textemdash\textemdash\textemdash} \tag{15}$$

After substituting for ρ its value $a\frac{\pi - \theta}{\sin\theta}$, and carrying through the integration,[9] equation (15) reduces to the simple form,

$$D = 2a\ p_n \frac{\sin^2\theta}{\pi - \theta}\bigg|_{\theta_1}^{\theta_2} \text{\textemdash\textemdash\textemdash\textemdash\textemdash\textemdash\textemdash\textemdash} \tag{16}$$

One observes from equation (16) that $D = 0$, as it should, when the limits of θ are 0 and π, that is when the integration extends over the whole surface of the half strut. Going aft from the bow the zonal drag sharply increases from zero to its maximum value at $x = \frac{a}{2}$, where the pressure is zero, and thereafter vanishes asymptotically.

---

[9] The step-by-step operations in this and subsequent integrations in this study are omitted. While for the most part the integrations are: straightforward, they are nevertheless tediously long and distracting. They have been omitted everywhere, therefore, for uniformity and brevity, even though a certain amount of mathematical continuity is sacrificed.

Surfaces of constant speed or pressure in the field about the half strut are found by solving equation (12) when a series of values is assigned to V. If one lets $V = KU$ equation (12) becomes,

$$U^2 (K^2 - 1) = \left(\frac{C}{\rho}\right)^2 \left(1 + 2\frac{\rho}{a}\cos\theta\right),$$

from which,

$$\rho^2 = \frac{a^2}{K^2-1} + \frac{2a\rho\ \cos\ \theta}{K^2-1} \quad\text{---}\quad (17)$$

If

$$\frac{a^2}{K^2-1} = r^2 - c^2, \text{ and } \frac{a}{K^2-1} = c,$$

equation (17) takes the form

$$\rho^2 = r^2 - c^2 + 2\ \rho\ c\ \cos\ \theta$$

which one recognizes as the equation of a family of circles whose centers are at points $(c, 0)$ and whose radii are the values assigned to r. The radii of the circles and the abscissas of their centers are simply

$$\left.\begin{array}{l} r = Kc \\[2mm] c = \dfrac{a}{K^2-1} \end{array}\right\} \quad\text{--}\quad (18)$$

It is interesting to note that the circle of infinite radius—that is the straight line—is the one for which $K = 1$, or for which V is the speed of the distant stream. This line crosses the bow at $x = \frac{a}{2}$ where the surface pressure is zero. The circles of constant speed or pressure are drawn from equations (18) in the upper half of Figure 6.

GRAPHICAL TREATMENT

Due to its simplicity, the whole treatment of the half strut has been carried through analytically. When one passes to the more complex distributions of sources and sinks, however, the analytical treatment becomes unmanageable, and graphical methods must be resorted to. For these more complicated cases the analytics can be carried without serious difficulty through the determination of the potential at any point of the flow field, but suddenly becomes unmanageable when the equation of the equipotential surfaces is required. Beginning therefore with the graphical determination of the streamlines, one of which is the strut surface, the determination of the velocity and pressure in such cases must be essentially graphical. In order to illustrate the method, it will be useful, to carry the simple case of the half strut through the first stages of the graphical treatment.

Beginning with equations (10), values of

$$\left.\begin{array}{ll} \dfrac{\psi_1{}'}{C} = -(\pi - \theta) = \tan^{-1}\dfrac{y}{x} - \pi, & x < 0 \\[3mm] \dfrac{\psi_1{}'}{C} = \theta \qquad\quad = \tan^{-1}\dfrac{y}{x}, & x > 0 \end{array}\right\}^{10} \quad\text{--------------------------------------}\quad (19)$$

are computed for various values of x and y, as listed in Table I and plotted in Figure 7. For a series of values of x one reads from this figure the values of $\frac{\psi_1{}'}{C}$ corresponding to the values of y chosen, and deducts from each value of $\frac{\psi_1{}'}{C}$ the half strength of the source divided by C when x
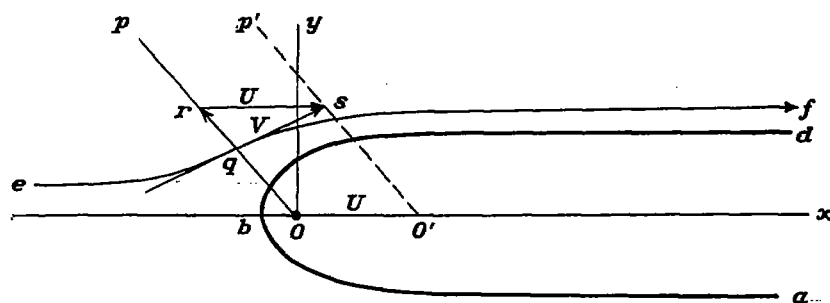
---

[10] The subscript, 1, indicates a source as distinguished from the subscript, 2, indicating a sink. The primes indicate that the stream function coefficients, $\frac{\psi}{C}$, have been reduced by the amount of the source-sink strength (divided by C) lying to the right, according to the first of equations (10), but not yet by the amount lying to the left, required by the second equation. When the latter deduction is made, the primes are omitted.

is positive, according to the second of equations (10). These values of $\frac{\psi_1}{C}$, with reversed sign, are then plotted against y giving curves of constant x, Figure 16.

Figure 16 is used to give two sets of streamlines, those of the source flow, in general it will be a source-to-sink flow, first alone, then combined with the uniform stream. The first are given by reading the values of y at which the x curves cross a given $\frac{\psi_1}{C}$ horizontal. In the case of the line source these streamlines are simply radii. The second are obtained by reading the values of y at which the x curves cross each of a series of straight parallel lines.

$$\frac{\psi_1}{C} = \frac{U}{C} y + n \triangle \frac{\psi}{C} \quad \text{(20)}$$

drawn across the figure as shown. The intersections of the x curves with the line through the origin—that is, with the line whose n in equation (20) is zero—are clearly solutions of equation (10) when ψ is zero. These intersections therefore determine the coordinates of points on the boundary curve $\psi = 0$, which is the surface of the half strut. Similarly the intersections with the lines $n = \pm 1, \pm 2, \pm 3$, etc., are the coordinates of successive streamlines (fig. 6) evenly graded from the boundary curve, outwardly when n is $(+)$ and inwardly when n is $(-)$.

FIGURE 2

The diagram, given in Figure 16, which is the key to the whole graphical solution, was devised and first used by Taylor. (Ref. 3.)

One defect of the diagram, just described is its failure to give the bow and stern points of the strut. These must be obtained by auxiliary use of the velocity potential ϕ. From equation (8)—

$$\frac{\partial \phi}{\partial x} = V_x = \frac{C}{x} + U$$

since $\rho = x$ when $y = 0$. But at the bow or stern $V_x = 0$, giving

$$\frac{U}{C} = -\frac{1}{x} \quad \text{(21)}$$

as the relation between the bow or stern position and the value of $\frac{U}{C}$. The hyperbola (21), is plotted in Figure 7.

The two sets of streamlines, those of the source flow, or in general those of the source-to-sink flow, first alone, then combined with the uniform stream, are drawn as in Figures 22 to 26. Let op Figure 2, be a typical streamline of the first set and ef a typical one of the second. At their intersection, q, which may be any point in the flow field, on, inside or outside the boundary surface abd, tangents to the streamlines can be drawn. These tangents, being coplaner with the direction of the uniform stream form two sides of a velocity triangle, qrs, whose third side is the constant horizontal velocity U. Three directions and one side being known, the resultant velocity V can be found.

A good graphical method for solving a set of these triangles at a number of qs along a streamline is the one used by Fuhrmann. At all the q points on a given streamline one draws on one of two sheets of transparent paper laid, for example, over Figure 22, the tangents to one set of streamlines, say the ef set, and on the other the tangents to the other set of streamlines, op. The two transparent sheets are then superimposed, one on the other, and displaced, relative to each

other, a distance U along x, so that the op set are in position $o'p'$ in Figure 2. The distances $qs = V$ are then read in succession simply by a scale, giving the resultant velocity along the stream-line in terms of the uniform stream speed U.

Finally knowing the velocity, the pressure for steady flow is given everywhere by equation (13). The pressures on the half-strut surface determined in this way agree with those given by equation (14).

<center>FIVE RANKINE STRUTS</center>

<center>THEORETICAL DEVELOPMENT</center>

In order to derive a series of Rankine struts whose shapes resemble the shape of struts used in aircraft, one needs a variety of distributed sources and sinks, particularly the latter. Following the treatment of the line source, the formulas for the stream function coefficient, $\frac{\psi_1'}{C}$, and for the velocity potential coefficient, $\frac{\varphi_1}{C}$, will therefore be found for surface sources having three types of strength distribution, the uniform, the linear, and the parabolic.

The three distributed types of sources require treatments which are sufficiently similar to justify developing all three together. Accordingly the equations in the following development will appear in triplets, the first of which is always for the uniformly distributed source, the second for the linearly distributed one, and the third for the parabolic. They will be distinguished in the development by the subscripts a, b, and c respectively, added to the equation numbers.

Consider a strip of width, l, cut from an infinite plane and beset uniformly with line sources running lengthwise. If the elementary line sources are equal in strength the strip is a uniformly distributed source; if they have strengths proportional to their distance from one edge of the strip, the source is a linearly distributed one, and if their strengths are proportional to the square of this distance, the source is parabolically distributed.[11] Let the total strength of the strip source

<center>FIGURE 3</center>

be $2\pi C$ per unit length along z. Then, clearly, an elementary strip, $d\xi$ (fig. 3) has the strengths, $2\pi C \frac{d\xi}{l}$, $2\pi C \frac{2\xi d\xi}{l^2}$, and $2\pi C \frac{3\xi^2 d\xi}{l^3}$, according as the distribution is uniform, linear or parabolic.

By equation (8) these elements at a distance ξ from the z axis, add to the velocity potential φ_1 at the point P, the values,

$$\frac{d\varphi_1}{C} = \frac{1}{l} \ln \rho \, d\xi,$$

$$= \frac{2}{l^2} \ln \rho \, \xi d\xi,$$

$$= \frac{3}{l^3} \ln \rho \, \xi^2 d\xi,$$

Substituting the value of ρ and writing in integral form, these equations become

$$\frac{\varphi_1}{C} = \frac{1}{2l} \int_0^l \ln \left[(x - \xi)^2 + y^2 \right] d\xi \text{------------------------------------- (22a)}$$

$$= \frac{2}{2l^2} \int_0^l \ln \left[(x - \xi)^2 + y^2 \right] \xi d\xi \text{------------------------------------ (22b)}$$

$$= \frac{3}{2l^3} \int_0^l \ln \left[(x - \xi)^2 + y^2 \right] \xi^2 d\xi \text{----------------------------------- (22c)}$$

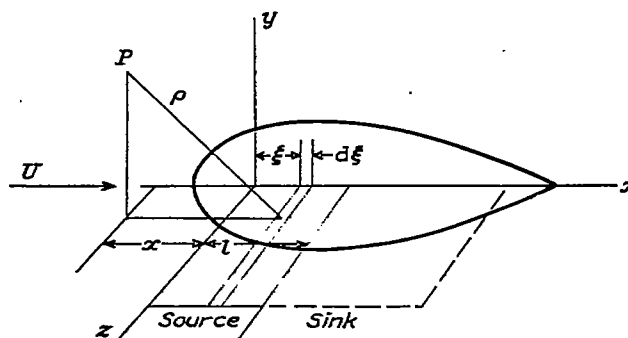[11] Fuhrmann, Reference 1, used only the uniform and linear strength distribution.

Values of $\frac{\varphi_1}{C}$ will be required only for the determination of the bow and stern points of the boundary surfaces for which $y=0$. Letting $y=0$ in equations (22), and integrating, one obtains,[12]

$$\frac{\varphi_1}{C}=\frac{1}{l}\left[(l-x)\ln(x-l)+x\ln x-l\right] \tag{23a}$$

$$=\frac{1}{l^2}\left[(l^2-x^2)\ln(x-l)+x^2\ln x-lx-\frac{l^2}{2}\right] \tag{23b}$$

$$=\frac{1}{l^3}\left[(l^3-x^3)\ln(x-l)+x^3\ln x-lx^2-\frac{l^2x}{2}-\frac{l^3}{3}\right] \tag{23c}$$

If equation (8) is differentiated partially with respect to x, we obtain the equation for the bow point,

$$V_x=\frac{\partial}{\partial x}\left(\frac{\varphi}{C}\right)=\frac{\partial}{\partial x}\left(\frac{\varphi_1}{C}\right)+\frac{U}{C}=0 \tag{24}$$

Differentiating equations (23) partially with respect to x and substituting in equation (24) one obtains,

$$\frac{U}{C}=\frac{1}{l}\left(\ln\frac{x-l}{x}\right) \tag{25a}$$

$$=\frac{2}{l^2}\left(x\ln\frac{x-l}{x}+l\right) \tag{25b}$$

$$=\frac{3}{l^3}\left(x^2\ln\frac{x-l}{x}+xl+\frac{l^2}{2}\right) \tag{25c}$$

These are the relations between the values of $\frac{U}{C}$ and the abscissas of the bow point, corresponding to equation (21) for the line source. The graphs of equation (25a), (25b), and (25c) are found in Figures 8, 9, and 10, respectively.

By equation (9) the elementary strip, $d\xi$, Figure 3, likewise adds to the stream function ψ_1', at the point P the values,

$$\frac{d\psi_1'}{C}=\frac{1}{l}\left(\tan^{-1}\frac{y}{x-\xi}-n\pi\right)d\xi,$$

$$=\frac{2}{l^2}\left(\tan^{-1}\frac{y}{x-\xi}-n\pi\right)\xi d\xi,$$

$$=\frac{3}{l^3}\left(\tan^{-1}\frac{y}{x-\xi}-n\pi\right)\xi^2 d\xi,$$

where $n=1$ if $x<0$ and $n=0$ if $x>0$. The whole stream function at P due to the source is therefore,

$$\frac{\psi_1'}{C}=\frac{1}{l}\int_0 \tan^{-1}\frac{y}{x-\xi}\,d\xi-L \tag{26a}$$

$$=\frac{2}{l^2}\int_0 \tan^{-1}\frac{y}{x-\xi}\,\xi d\xi-M \tag{26b}$$

$$=\frac{3}{l^3}\int_0 \tan^{-1}\frac{y}{x-\xi}\,\xi^2 d\xi-N \tag{26c}$$

---

[12] The integrated forms of equations (22a) and (22b), when y is retained, are

$$\frac{\varphi_1}{C}=\frac{1}{l}\left\{\frac{1}{2}(l-x)\ln[(x-l)^2+y^2]+\frac{x}{2}\ln(x^2+y^2)-l-y\left(\tan^{-1}\frac{x-l}{y}-\tan^{-1}\frac{x}{y}\right)\right\} \tag{23'a}$$

$$-\frac{1}{2l^2}\{[(x-l)^2+y^2]\ln[(x-l)^2+y^2]-[(x-l)^2+y^2]-(x^2+y^2)\ln(x^2+y^2)+(x^2+y^2)\}+\frac{2x}{l}H. \tag{23'b}$$

where $H=\frac{\varphi_1}{C}$ for the uniform source given in equation (23'a).

The values chosen for y were, for all, $+1, +2, +3, +4, +5, +6, +8, +10, +12, +14$. The values chosen for x were in equation (28a), $+5, +7, +9, +10, +11, +13, +16, +20, +25, +30, +35, +40, +50$; in equation (28b), for $l=5, -40, -35, -30, -25, -20, -16, -13, -10, -7, -5, -2, 0, +2, +4, +5, +6, +8, +11, +13, +16, +20, +25, +30, +35, +40, +50$; for $l=20, -40, -35, -36, -25, -20, -16, -13, -10, -3, -5, -2, 0, +2, +5, +7, +10, +13, +16, +18, +20, +22, +25, +30, +35, +40, +50$; in equation (28c), $-40, -35, -30, -25, -20, -16, -13, -10, -7, -5, -2, 0, +3, +5, +7, +9, +10, +11, +13, +16, +20, +25, +30, +35, +40, +50$.

where,

$$L = \pi \left(1 - \frac{\xi}{l}\right) \quad \text{(27a)}$$

$$M = \pi \left(1 - \frac{\xi^2}{l^2}\right) \quad \text{(27b)}$$

$$N = \pi \left(1 - \frac{\xi^3}{l^3}\right) \quad \text{(27c)}$$

is the amount of the source half strength downstream, or to the right of ξ.

Equations (26) integrate to the equations,

$$\frac{\psi_1'}{C} = \frac{1}{l}\left[x \tan^{-1}\frac{y}{x} - (x-l)\tan^{-1}\frac{y}{x-l} + \frac{y}{2}\ln\frac{x^2+y^2}{(x-l)^2+y^2}\right] - L \quad \text{(28a)}$$

$$\frac{\psi_1'}{C} = \frac{1}{l^2}\left[(x^2-y^2)\tan^{-1}\frac{y}{x} - (x^2-y^2-l^2)\tan^{-1}\frac{y}{x-l} - ly + xy\ln\frac{x^2+y^2}{(x-l)^2+y^2}\right] - M \quad \text{(28b)}$$

$$\frac{\psi_1'}{C} = \frac{1}{l^3}\left[3x^2 I_1 - 3x I_2 - (x-l)^3 \tan^{-1}\frac{y}{x-l} + x^3 \tan^{-1}\frac{y}{x} - \frac{yl}{2}(l-2x)\right.$$
$$\left. - \frac{y^3}{2}\ln\frac{x^2+y^2}{(x-l)^2+y^2}\right] - N \quad \text{(28c)}$$

where I_1 is the bracket term in equation (28a) and I_2 is the bracket term in equation (28b). Values of $\frac{\psi_1'}{C}$ have been computed from equations (28) for 10 values of y, for each of 13 values of x, in the case of the symmetrical distribution, (28a), and for each of 26 values of x in the case of (28b) and (28c), and all for $l=10$, in (28a) and (28c) and $l=5$ and $l=20$ in (28b).[12] The values of the stream function coefficients, $\frac{\psi_1'}{C}$, for the three distributed sources are given in Tables II, III, and IV and plotted in Figures 8, 9, and 10.

The corresponding sink strips produce potential coefficients of like magnitude but of opposite sign. One has therefore only to change the sign of C from positive to negative in equations (19) to (28) and in the corresponding figures to obtain the stream function coefficients and the values of $\frac{U}{C}$ for the four types of distributions when used as sinks. The stream function coefficient of a sink is denoted $\frac{\psi_2'}{C}$.

The combined coefficient of a source and sink, when both are equal in strength, is clearly $\frac{\psi_1' + \psi_2'}{C}$ which one obtains for any point in the flow field by simply adding the two stream function coefficients produced there by the two independent flows. By carefully adding coefficients taken from Figures 7 to 10 in a routine way, Figures 11 to 15 have been constructed, giving the stream function coefficients and the values of $\frac{U}{C}$ for the five source-sink combinations represented diagramatically in Figure 4.

The five combinations contain two series of three each, one series has a common source combined with three types of sinks, the other has a common sink combined with three types of sources. Combinations I, II, III make up the first series, II, IV, V the second. It will be observed that no combinations are used giving vanishing source or sink strengths at the combined strip edges, such as would result, for example, by rotating the sink in combination III through an angle π about z at its mid-length. The edge of vanishing strength in such a combination produces a cusp at the bow or stern of the boundary surface. The surface then departs too far from forms of high merit to justify its study. This contrasts with the three dimensional case in which source-sink combinations having vanishing strengths at the ends produce boundary surfaces of revolution free of cusps and of good airship form. (Ref. 1.)

[12] See footnote on p. 732.

Equations (28) and their corresponding diagrams, Figures 8, 9, and 10, as well as the five combination diagrams, Figures 11 to 14, give the stream function coefficients corrected only for that part of the source-sink strength lying downstream. The physical interpretation of these diagrams is clear.

Upon superimposing a uniform field on these source-sink fields the second deduction must be made. The amount of the source-sink strength upstream (divided by C), must be deducted from each value of $\frac{\psi_1' + \psi_2'}{C}$ giving values of $\frac{\psi_1 + \psi_2}{C}$, as explained in connection with equation (10). These deductions, however, are very simple ones to make. If the ordinate to the point in the field, where the value of $\frac{\psi_1 + \psi_2}{C}$ is desired, stands on the source strip, the deduction may be read from graphs of equations (27). If the ordinate stands on the sink strip, one uses the relation that the strength upstream is the same as that downstream, with reversed sign, and obtains the deduction by reading the values as before from graphs of equations (27) but reversing the sign. After applying these deductions one obtains the same values of $\frac{\psi_1 + \psi_2}{C}$ as would have been obtained had equation (9) been used and no deductions made. From this point on, the developments proceeding from equations (9) and (10) are the same.

One next plots against y, the values of $\frac{\psi_1 + \psi_2}{C}$, just obtained, giving a family of curves of constant x, for each of the five combinations. The diagrams so obtained are shown in Figures 17 to 21 and correspond to Figure 16 for the half strut, whose use has already been explained. In each diagram, the straight line,

$$\frac{\psi}{C} = \frac{U}{C}y \quad \text{-- (29)}$$

through the origin, is so sloped as to intersect the uppermost x curve at a value of y which is the desired half-thickness of the strut. To obtain the strut half thickness, the width and fineness ratio [13] must be known. The width is known approximately from the total strip width of the source-sink combination. The fineness ratio was made approximately 3.5 which is common in practice.[14] Having obtained the slopes, one draws across Figures 17 to 21 a series of parallels $\frac{\psi}{C} = \frac{U}{C}y + n\Delta\frac{\psi}{C}$ graded from the line $\frac{\psi}{C} = \frac{U}{C}y$ by integral multiples of $\Delta\frac{\psi}{C}$, just as was done in Figure 16 for the half strut.

Following the treatment of the half strut, the horizontals in Figures 17 to 21 give values of x, y which enable one to draw point by point the source-to-sink streamlines, $\frac{\psi_1 + \psi_2}{C} = \text{const.}$ These are drawn in the upper half of Figures 22 to 26. Similarly, the sloping parallels give values of x, y from which one draws the resultant flow streamlines $\frac{\psi}{C} = \text{const.}$, one being the strut form itself. These latter are drawn in the lower half of the figures. The values of x, y giving the strut surface and including the bow and stern points obtained from the $\frac{U}{C}$ curves of Figures 11 to 15 are given in Table V for each of the five struts.

---

[13] The fineness ratio is the ratio of the strut width and maximum thickness.

[14] If one changes the slope of the line by assigning a series of values to $\frac{U}{C}$ equation (29), a series of struts of varying fineness ratio is obtained.
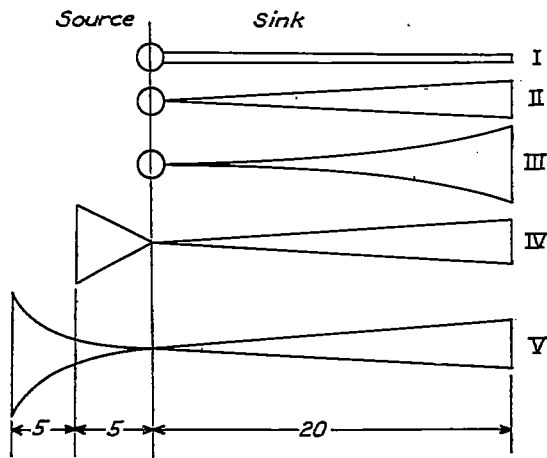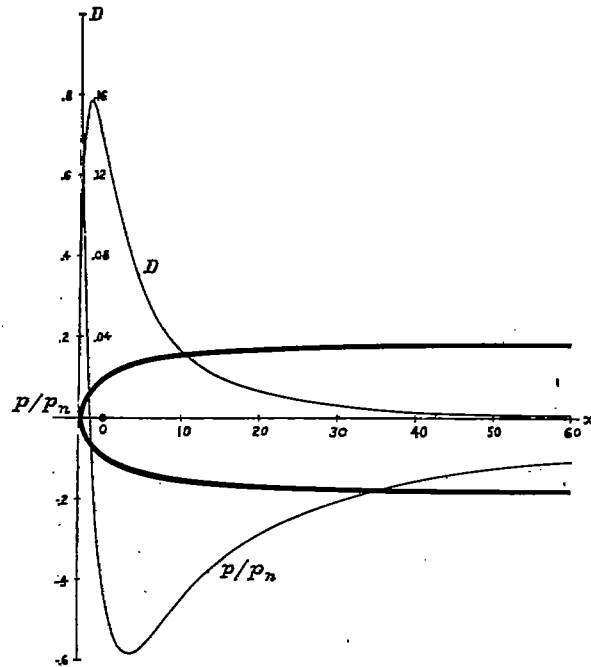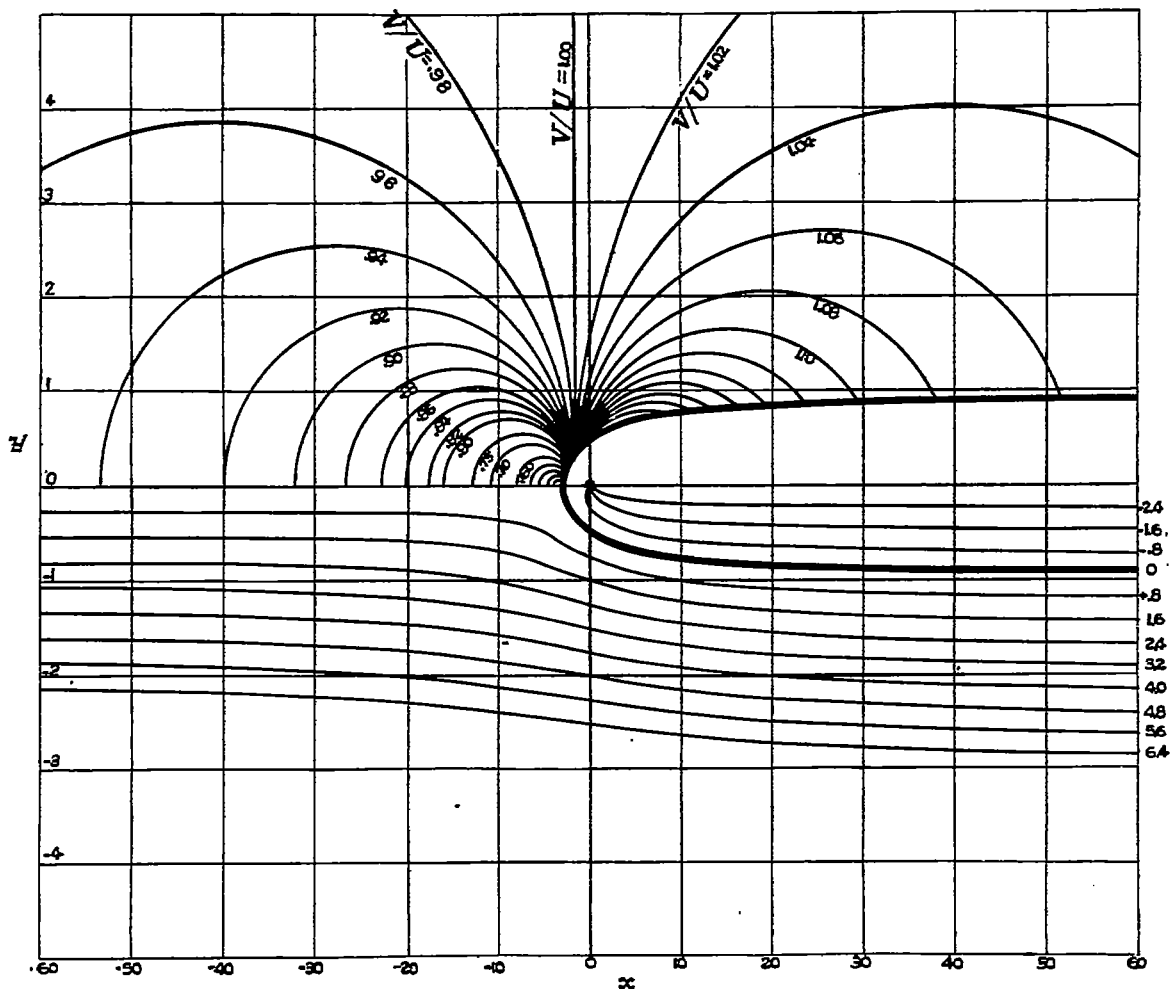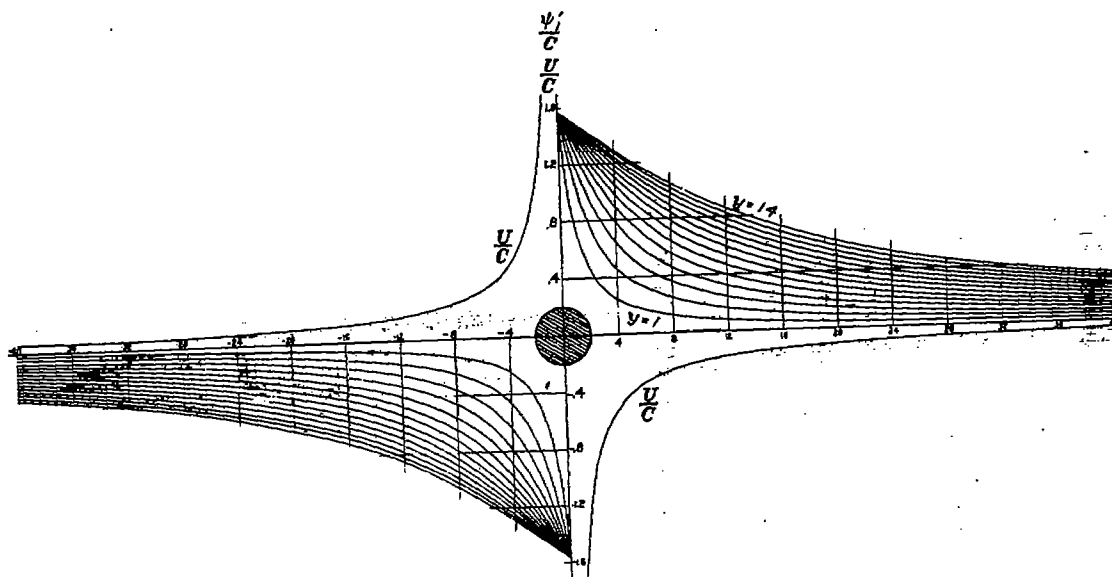
FIGURE 4

FIGURE 5.—Surface pressure and zonal drag of half strut formed by a line source in uniform stream. D in pounds per foot run at 40 miles per hour, standard inviscid air

FIGURE 6.—Circles of constant speed and resultant streamlines for the half strut formed by a line source in a uniform inviscid stream

FIGURE 7.—$\frac{\psi'}{C}$ diagram for the line source
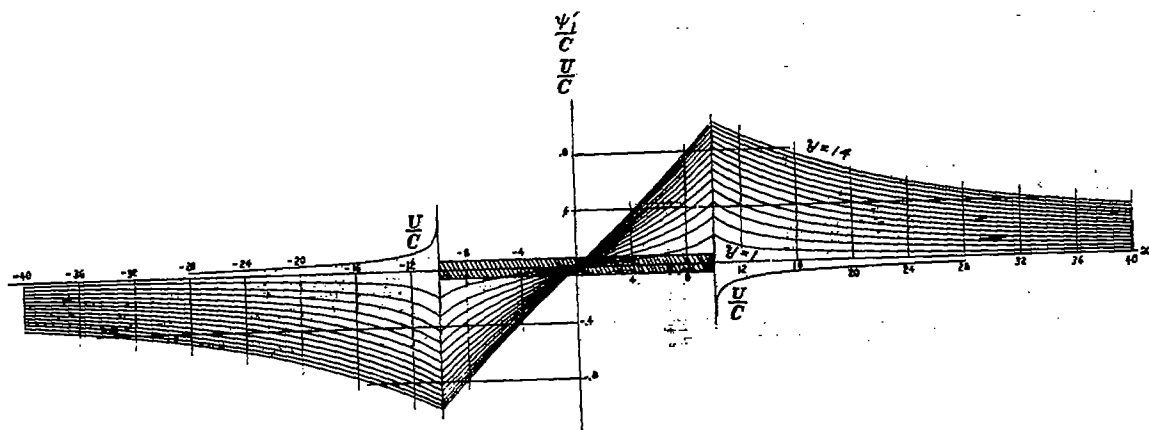
FIGURE 8.—$\frac{\psi'}{C}$ diagram for the surface source of uniform intensity
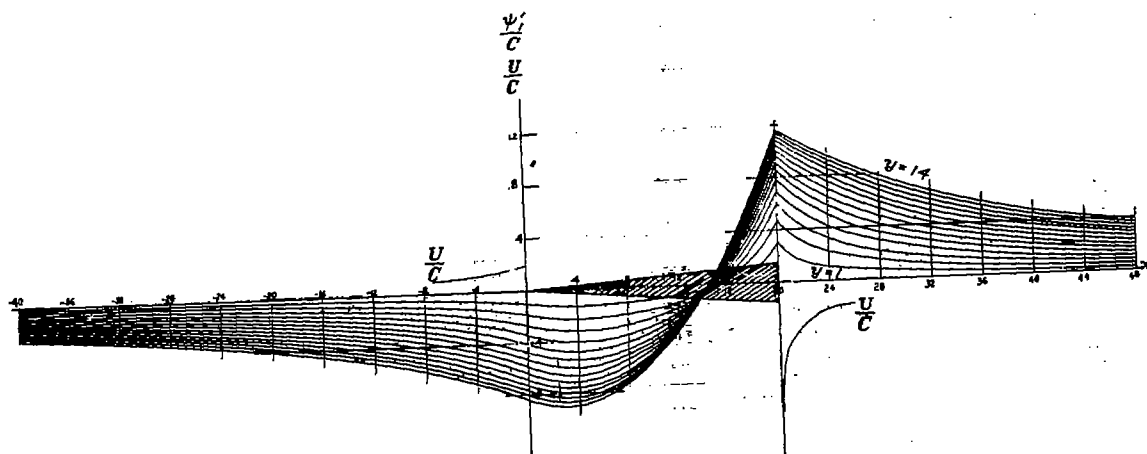
FIGURE 9.—$\frac{\psi'}{C}$ diagram for the surface source of linearly increasing intensity

Having constructed Figures 22 to 26, one obtains the velocity, and from the velocity the pressure along any streamline by the method explained in the treatment of the half strut. The velocity and pressure found at the surface of the five struts are listed in Tables VI to X. Finally
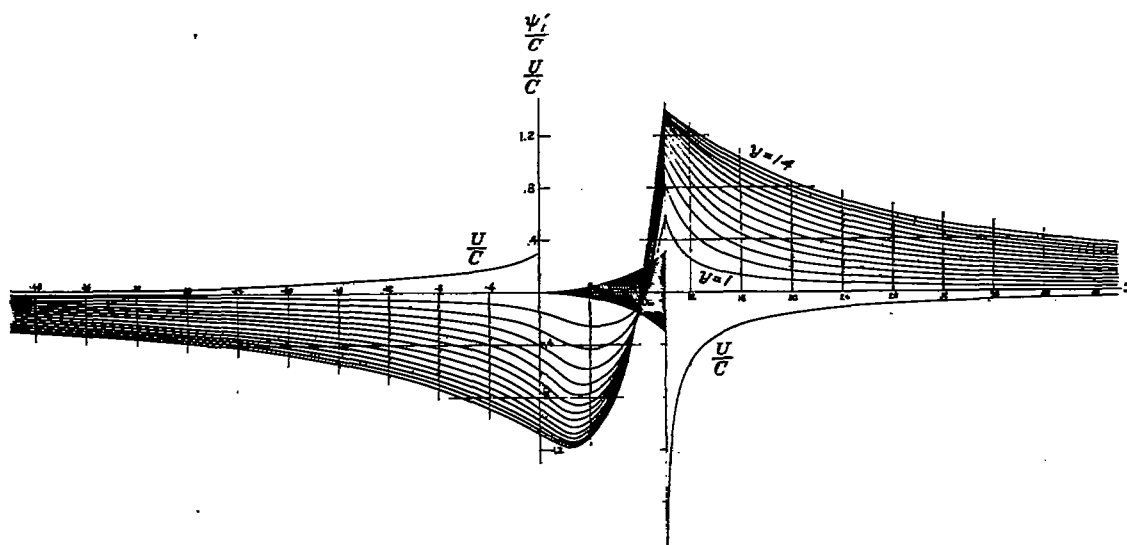
FIGURE 10.—$\frac{\psi'}{C}$ diagram for the surface source of parabolically increasing intensity

the pressures are plotted against strut width in Figures 27 to 31 and against strut half-thickness for integration in Figures 32 to 36.

The theoretical resistance of each strut in inviscid air is the integrated pressural drag which is proportional to the difference between the areas a, b, g, e, f, and g, c, g of the theoretical pres-
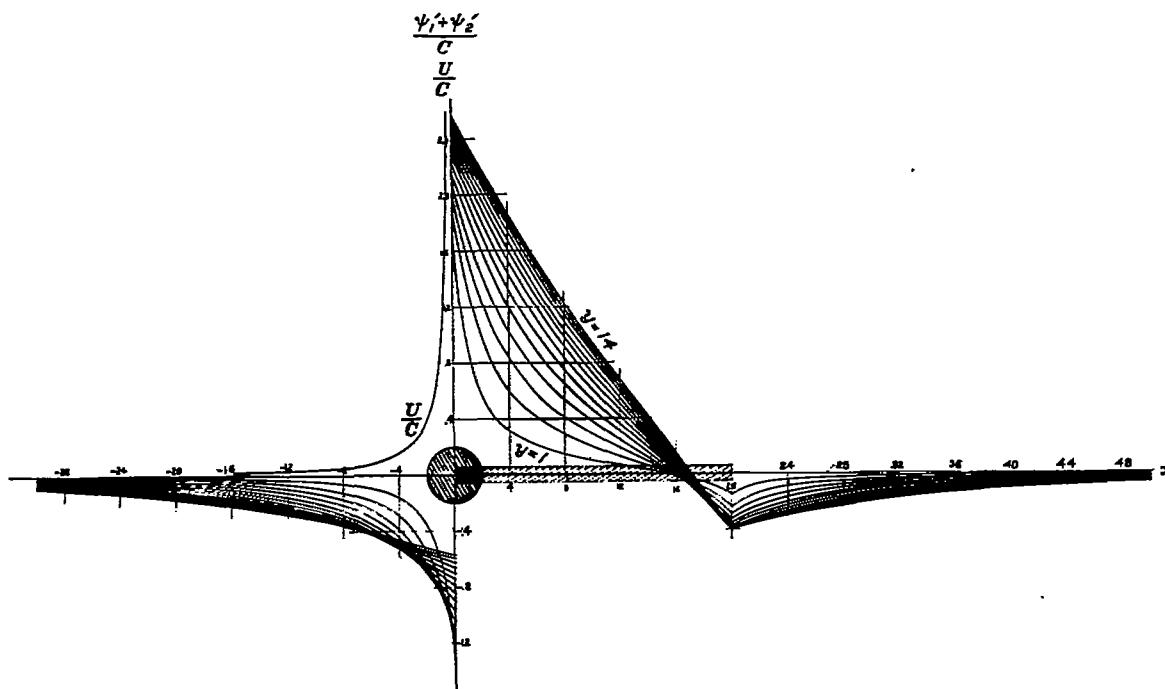
FIGURE 11.—$\frac{\psi'_1 + \psi'_2}{C}$ diagram for the source-sink combination No. I, Figure 4

sure curves in Figures 32 to 36. Since the theoretical resistance should be nothing, the areas should be equal. When the two areas for each strut are integrated they are found to be equal within the precision of the development. The magnitudes of the four components of pressure

FIGURE 12.—$\dfrac{\psi_1'+\psi_2'}{C}$ diagram for the source-sink combination No. II, Figure 4
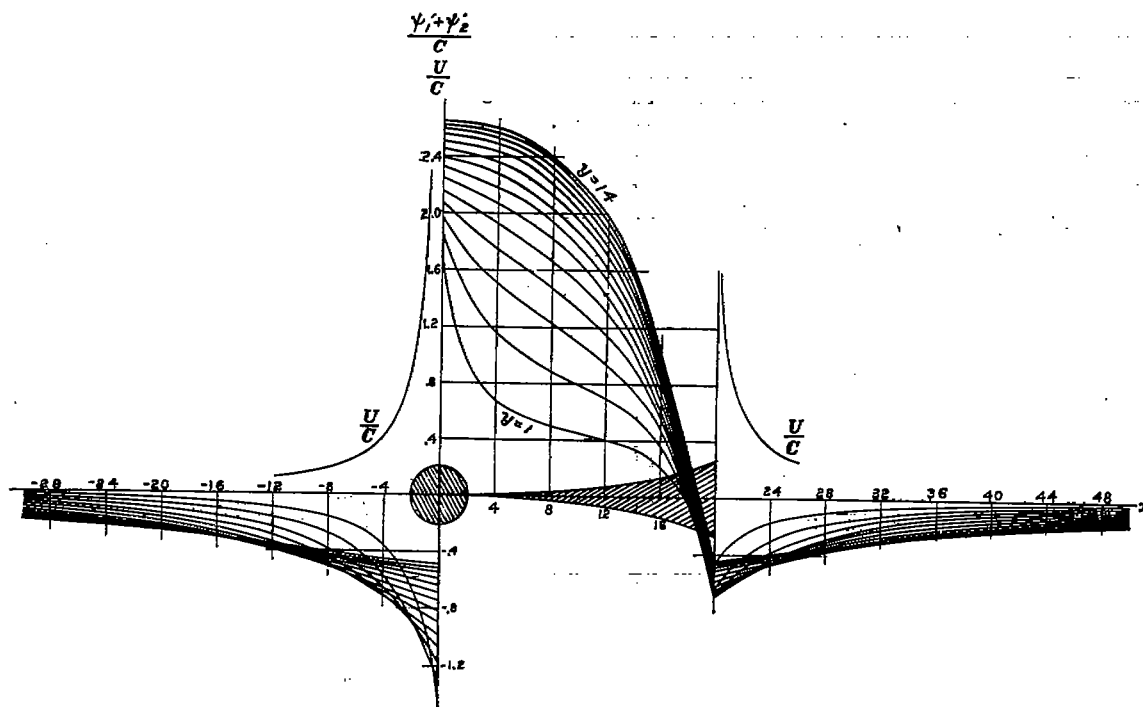
FIGURE 13.—$\dfrac{\psi_1'+\psi_2'}{C}$ diagram for the source-sink combination No. III, Figure 4

drag alongstream, which are the upstream and downstream push and suction, are given for both theory and experiment in Table XII.[15] The determination of the pressure distribution over the surface of the five struts completes the theoretical part of the study.
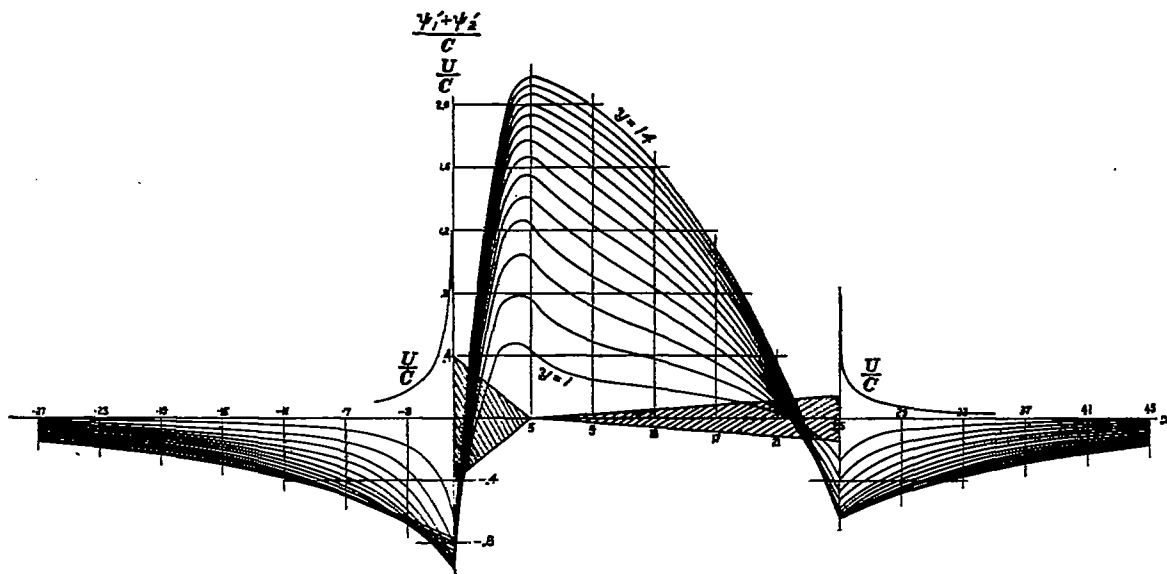
FIGURE 14.—$\frac{\psi'_1+\psi'_2}{C}$ diagram for the source-sink combination No. IV, Figure 4

EXPERIMENTAL RESULTS [16]

In order to compare the theoretical surface speeds and pressures with the actual ones in the case of air, models of the five theoretical struts were made and each subjected to resistance and pressure distribution tests in a wind tunnel. Along with these five, three empirical struts
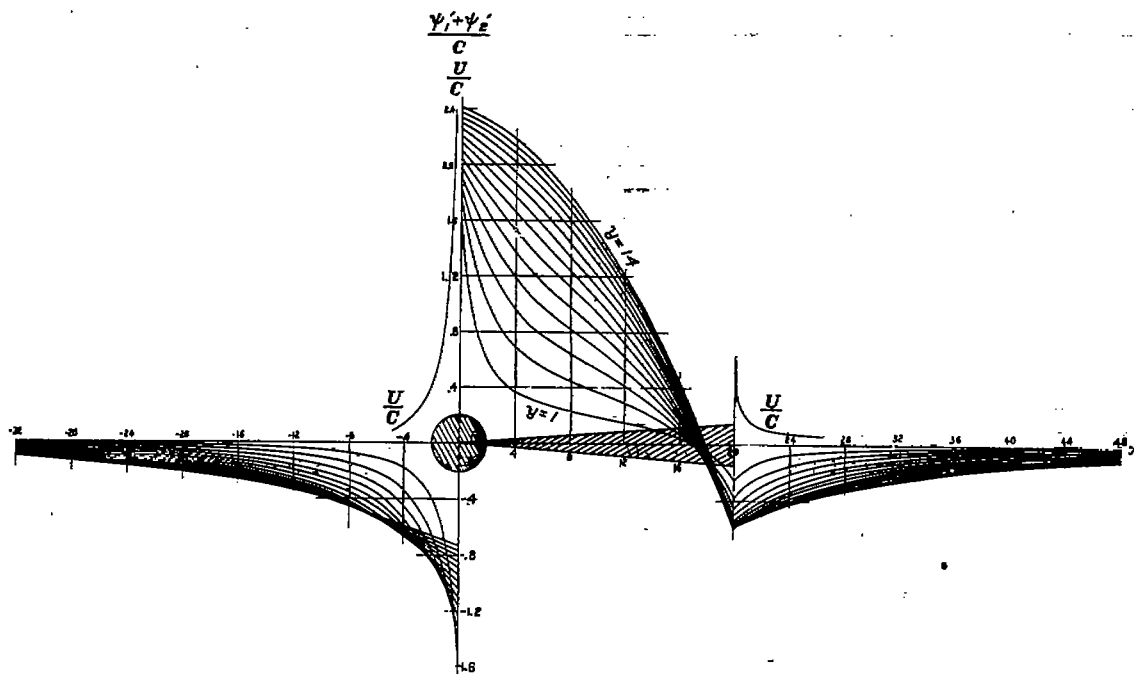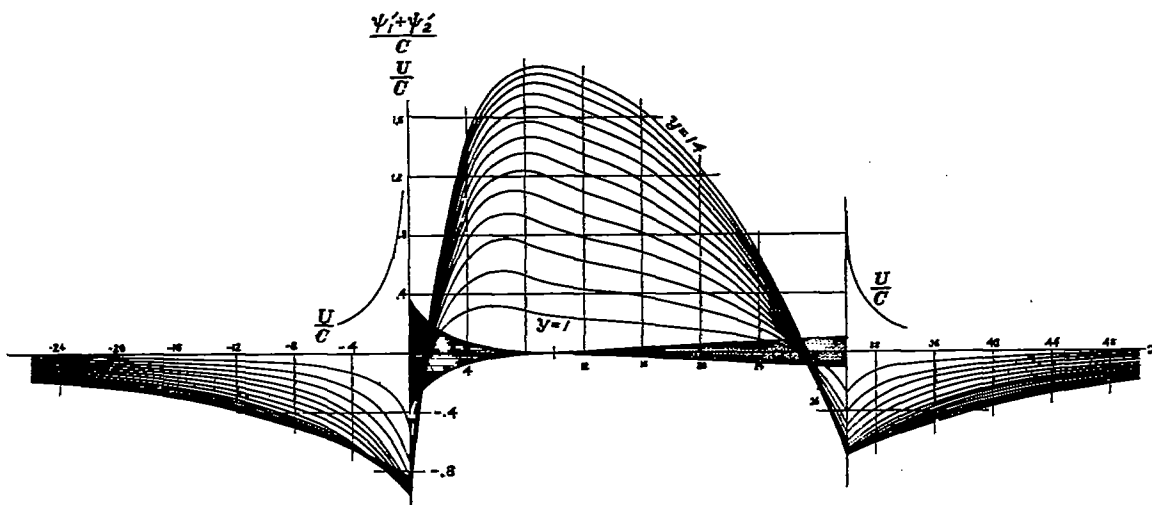

FIGURE 15.—$\frac{\psi'_1+\psi'_2}{C}$ diagram for the source-sink combination No. V, Figure 4

of high repute were made, one British, one German, and one American, and their resistances determined for comparison. The remaining part of the study will be devoted to a description of the models and to an analysis of the experimental results.

---

[15] The method used in Table XII of analyzing into its various components the resistance of a body moving through a fluid is due to Zahm. (Ref. 2.)

[16] See opening paragraph under "Experimental Investigation of U. S. Navy No. 2 strut," Part I. (Ref .10.)
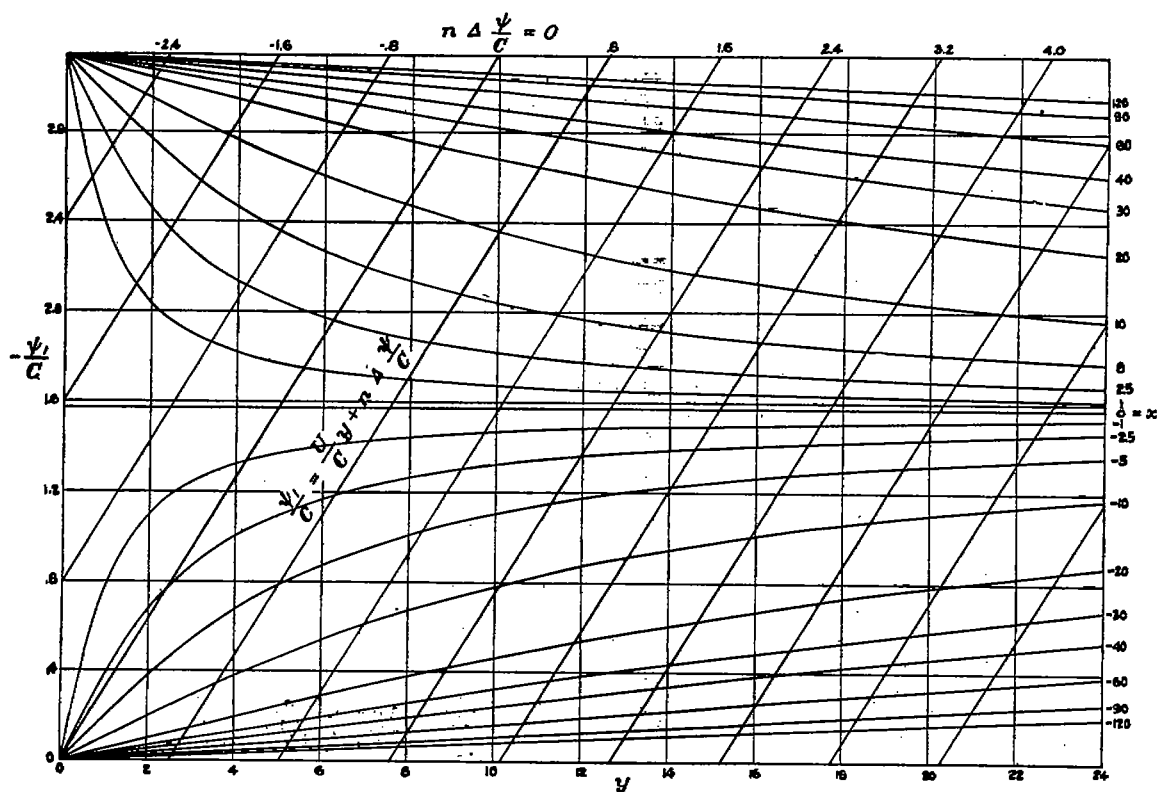
FIGURE 16.—$\frac{\psi_1}{C}$ diagram for the line source
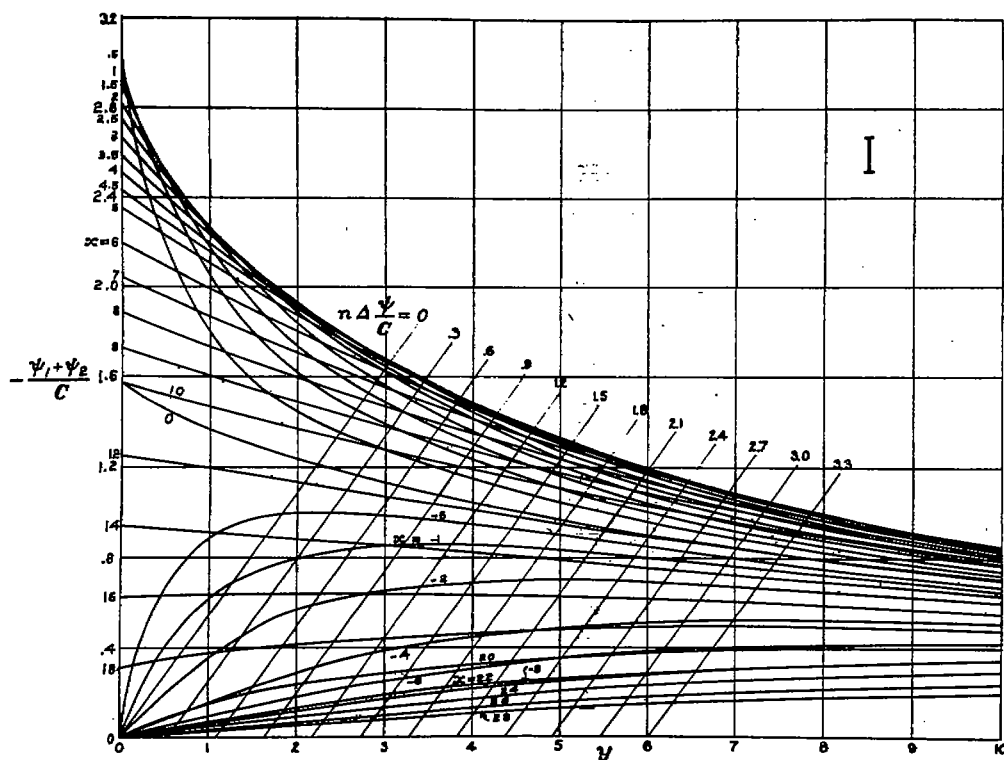
FIGURE 17.—$\frac{\psi_1+\psi_2}{C}$ diagram for the source-sink combination No. I, Figure 4
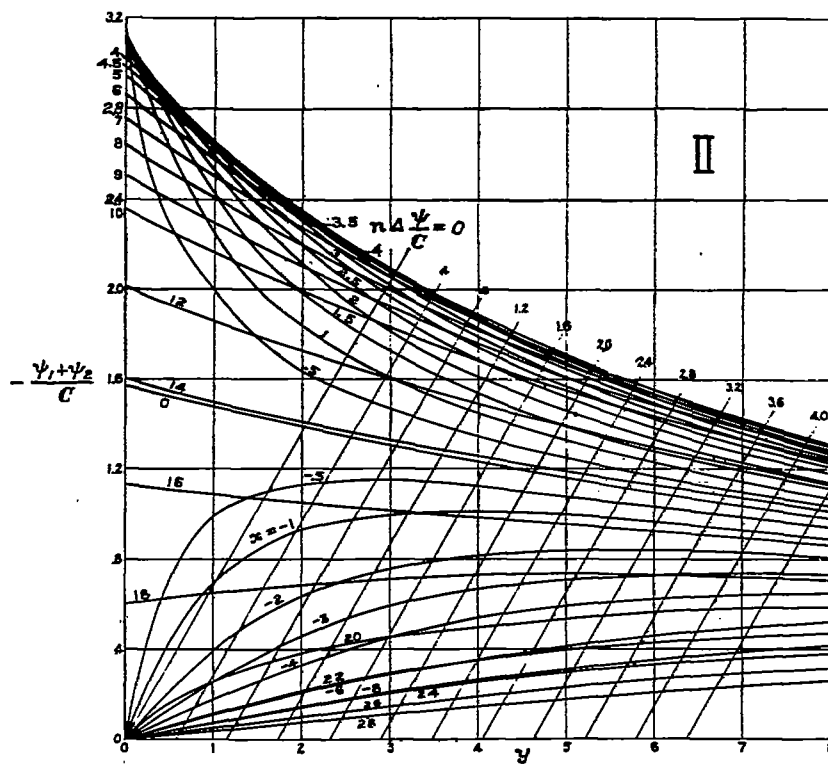
FIGURE 18.—$\dfrac{\psi_1+\psi_2}{C}$ diagram for the source-sink combination No. II, Figure 4
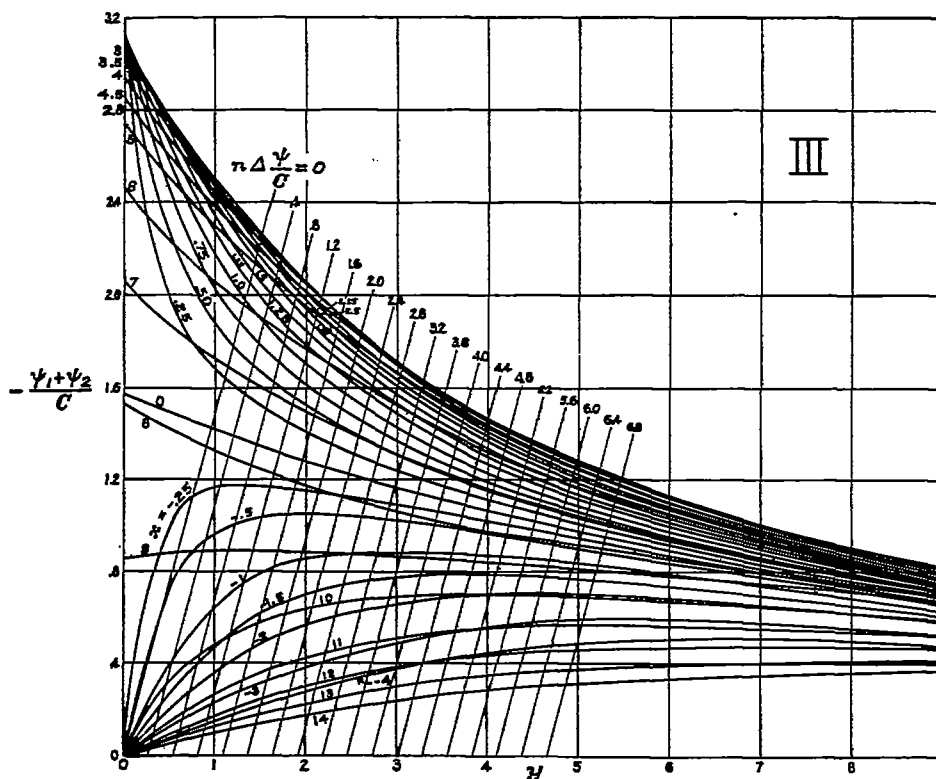
FIGURE 19.—$\dfrac{\psi_1+\psi_2}{C}$ diagram for the source-sink combination No. III, Figure 4
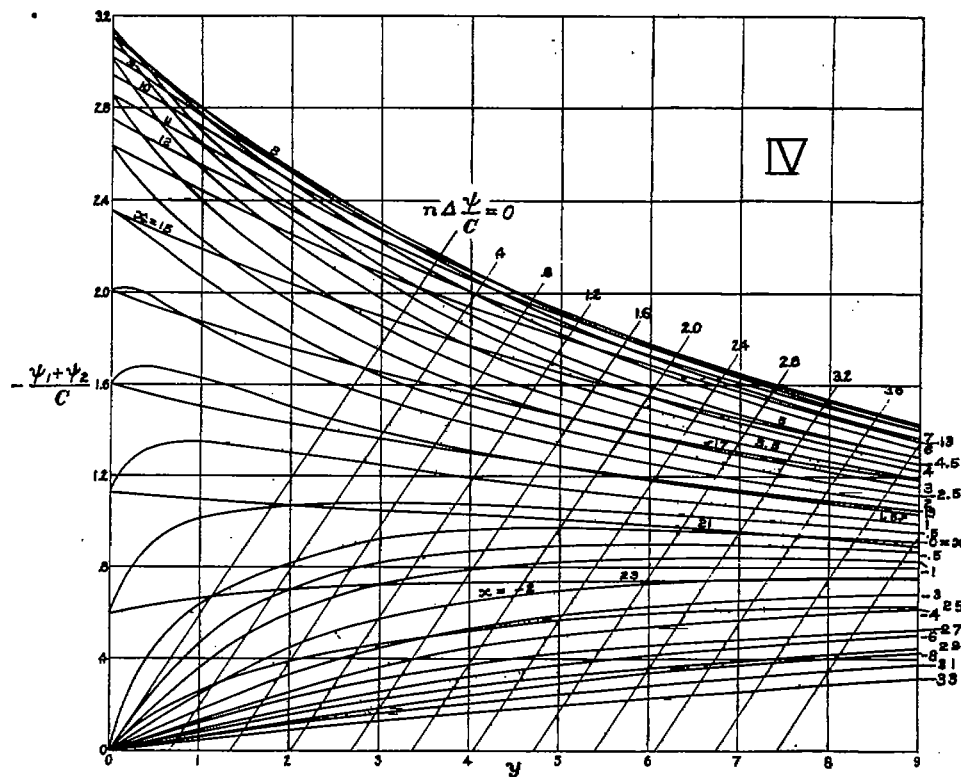
FIGURE 20.—$\dfrac{\psi_1 + \psi_2}{C}$ diagram for the source-sink combination No. IV, Figure 4
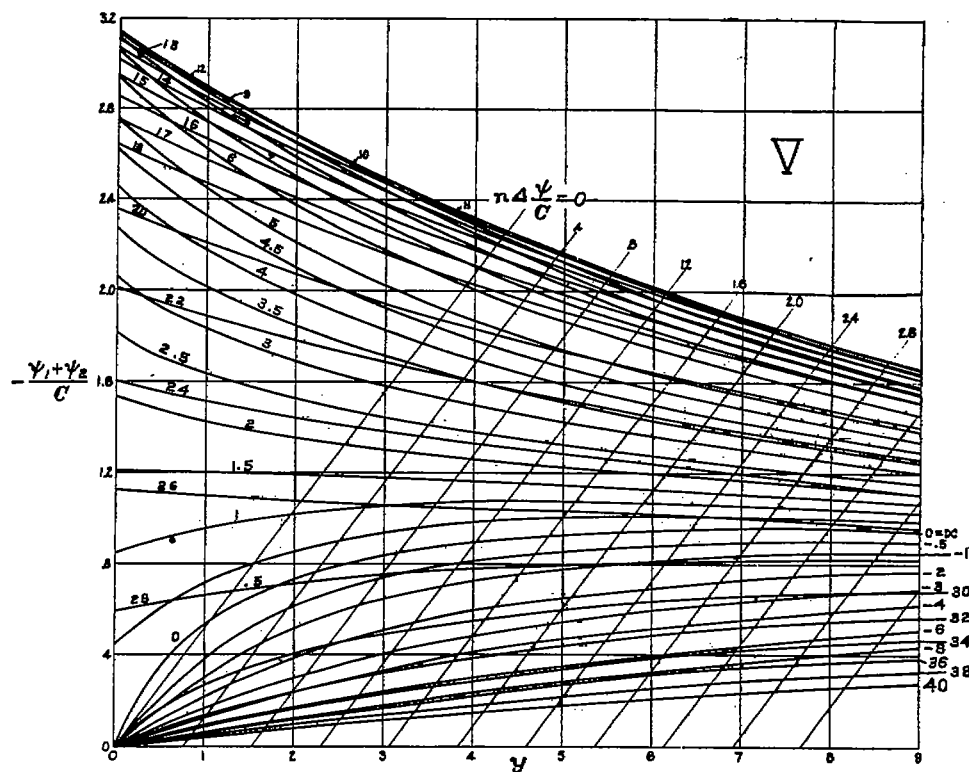
FIGURE 21.—$\dfrac{\psi_1 + \psi_2}{C}$ diagram for the source-sink combination No. V, Figure 4

APPARATUS AND EXPERIMENTAL METHOD

The wind tunnel used for these experiments was the United States Navy closed-circuit tunnel in Washington, which is equipped for force and moment measurement with Zahm's 6-component balance described in Reference 4. The test section of this tunnel is normally eight feet square and when so arranged the tunnel is capable of maintaining air speeds well
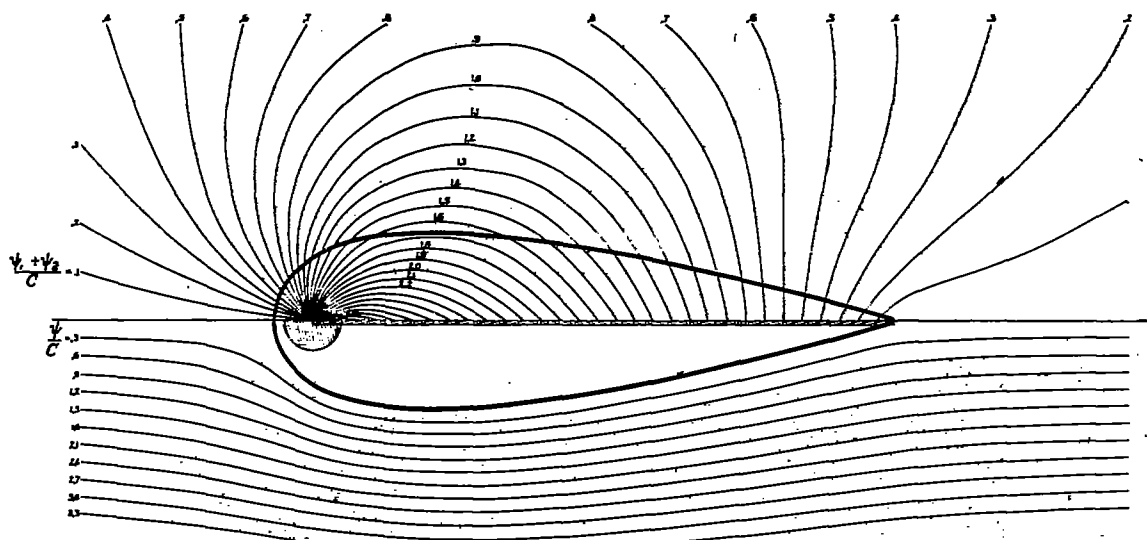
FIGURE 22.—Strut No. I, with source-to-sink and resultant streamlines

above 60 miles per hour whose mean values are controllable within one-half of 1 per cent. The balance is capable of measuring an air force or moment of a thousandth of a pound or pound-inch. The manometer from which the surface pressures were read was a single straight glass tube inclined approximately 1 to 10 and connected to an alcohol cistern. Its readings in vertical
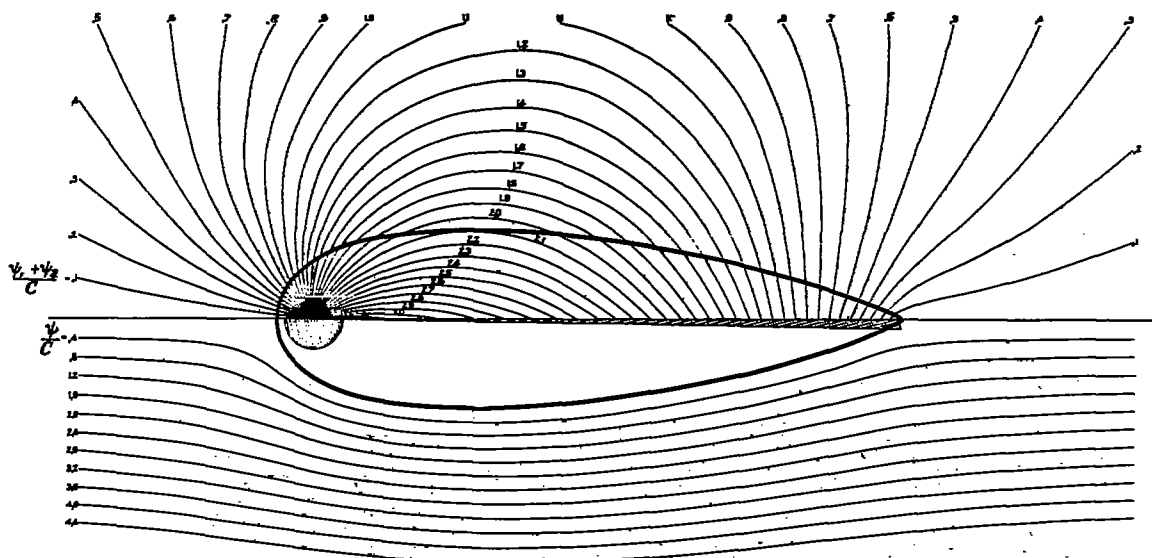
FIGURE 23.—Strut No. II, with source-to-sink and resultant streamlines

inches of water were carefully obtained by calibrating it against a water gauge capable of indicating pressures smaller than a thousandth inch of water.

The total resistance of each strut was obtained by attaching it to the 6-component balance which weighed its drag directly. The attaching holder was a thin 2-prong member whose

5-inch streamline prongs entered the strut at midspan as illustrated in Figure 37. Large separately supported end plates shielded the strut ends in both the resistance and the surface pressure tests as shown in Figures 37 and 38. These plates had the effect of making the strut a segment of a strut infinitely long and therefore of making the experimental conditions two
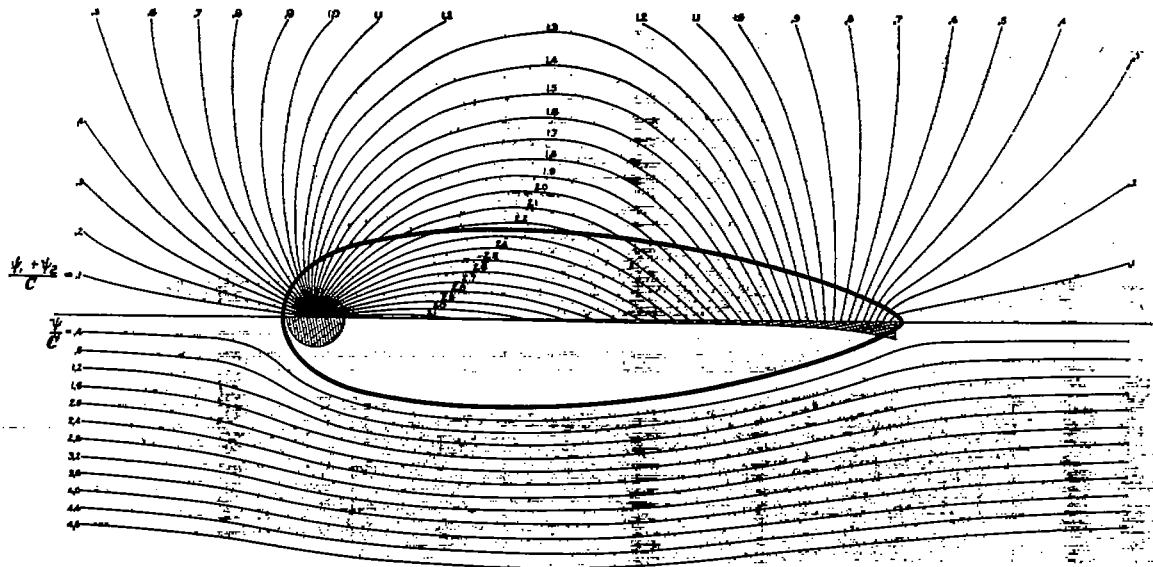
FIGURE 24.—Strut No. III, with source-to-sink and resultant streamlines

dimensional. No correction to the measured resistance was required, due to the pressure gradient along the tunnel, since the gradient is zero at the test section.

The pressure at each surface point was measured relative to the bow pressure by connecting the two differentially across the single-tube manometer.[17] The air speed of the general air
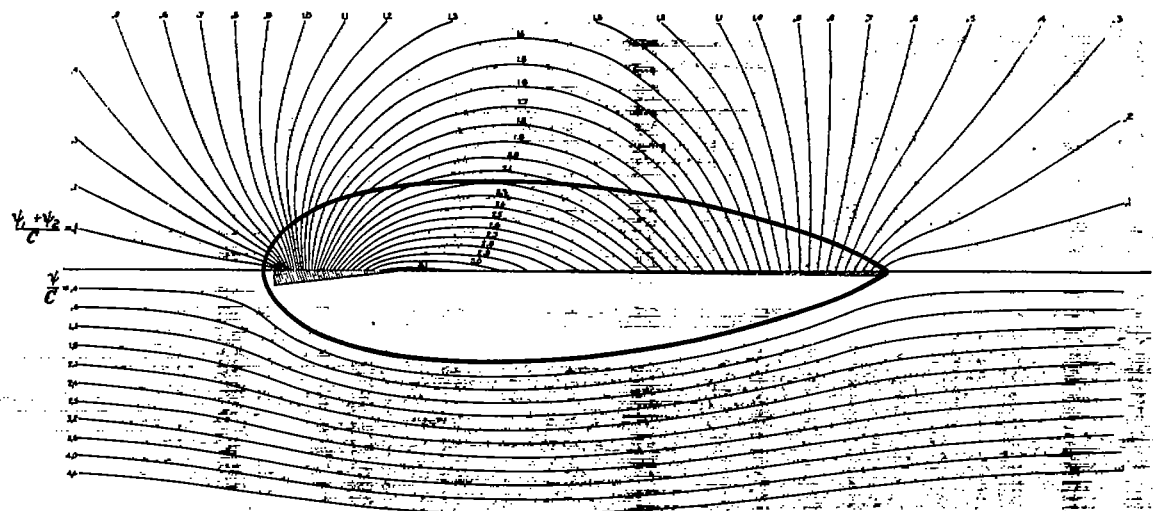
FIGURE 25.—Strut No. IV, with source-to-sink and resultant streamlines

stream was obtained by connecting the bow pressure and the static pressure of the distant air stream differentially across the speed indicating manometer. The static pressure of the stream was collected from the lateral perforations of a standard pitot-static tube placed sufficiently far abreast the bow of the strut to escape appreciable interference.

[17] When the forward rest point is known it furnishes a convenient and accurate reference for pressure elsewhere on the surface, since the pressure there is always $\frac{1}{2}\rho V^2$.
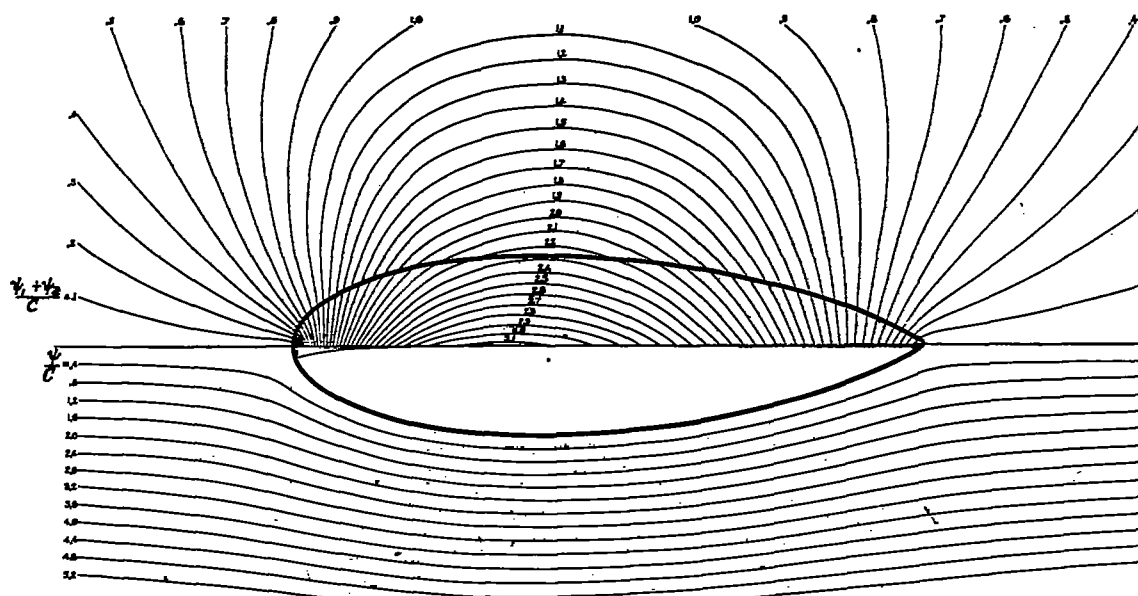
FIGURE 26.—Strut No. V, with source-to-sink and resultant streamlines
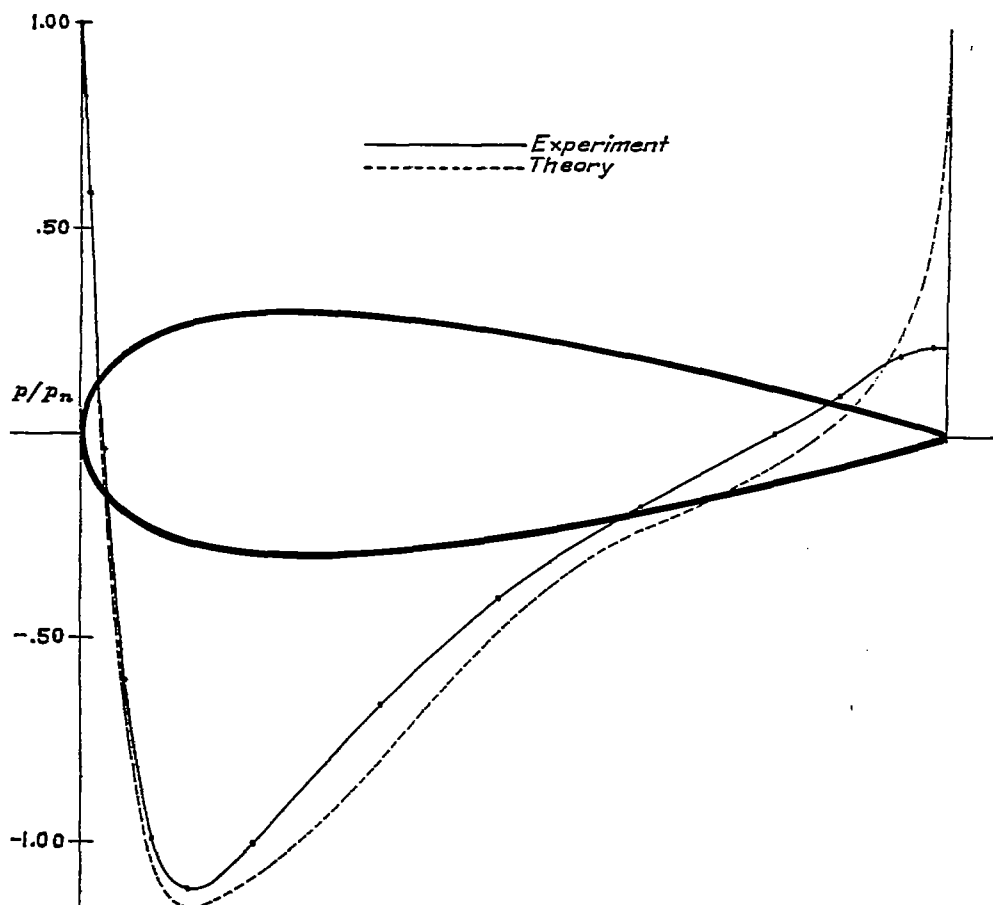
FIGURE 27.—Experimental and theoretical point pressure, p/p_n, over surface of strut No. I
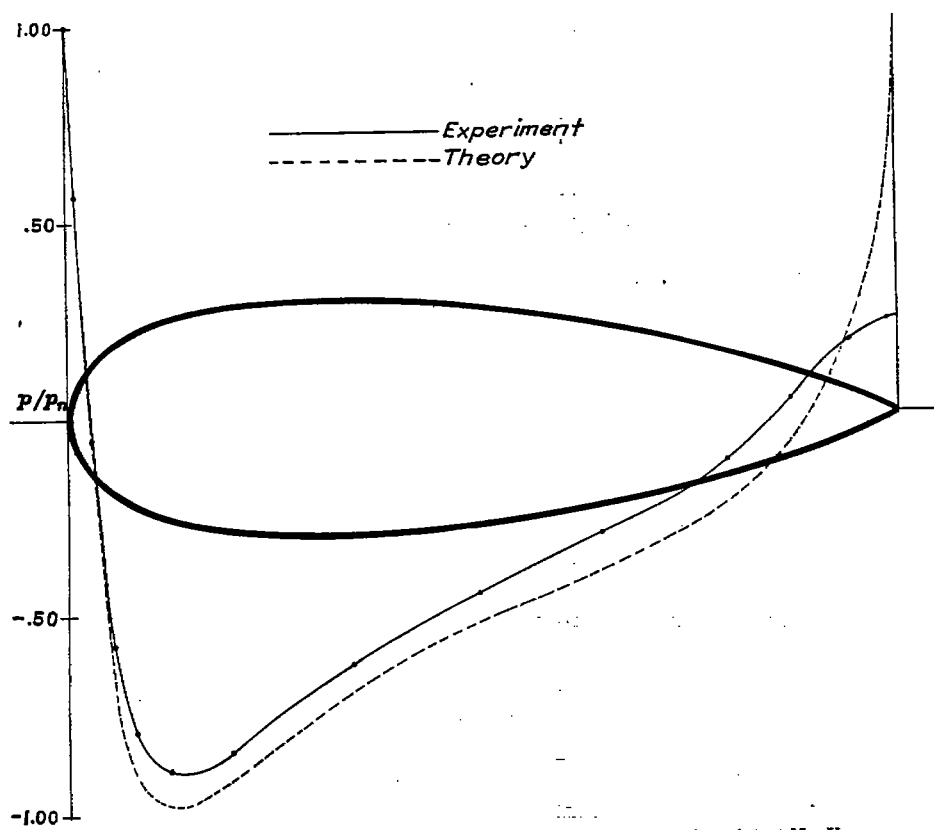
FIGURE 28.—Experimental and theoretical point pressure, p/p_n, over surface of strut No. II
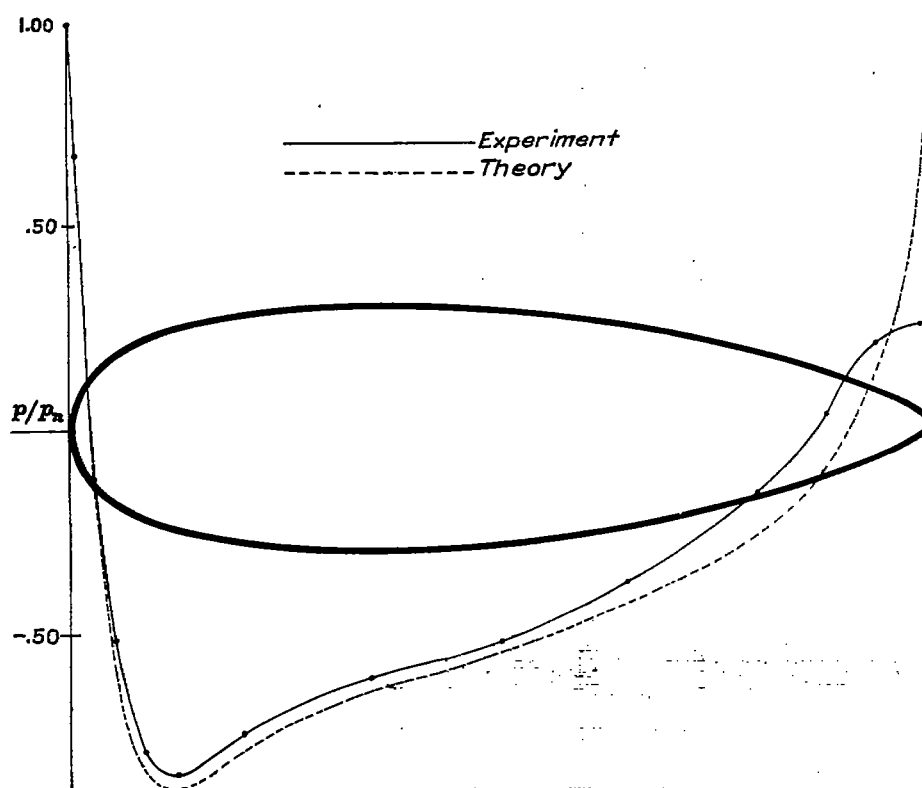
FIGURE 29.—Experimental and theoretical point pressure, p/p_n, over surface of strut No. II.
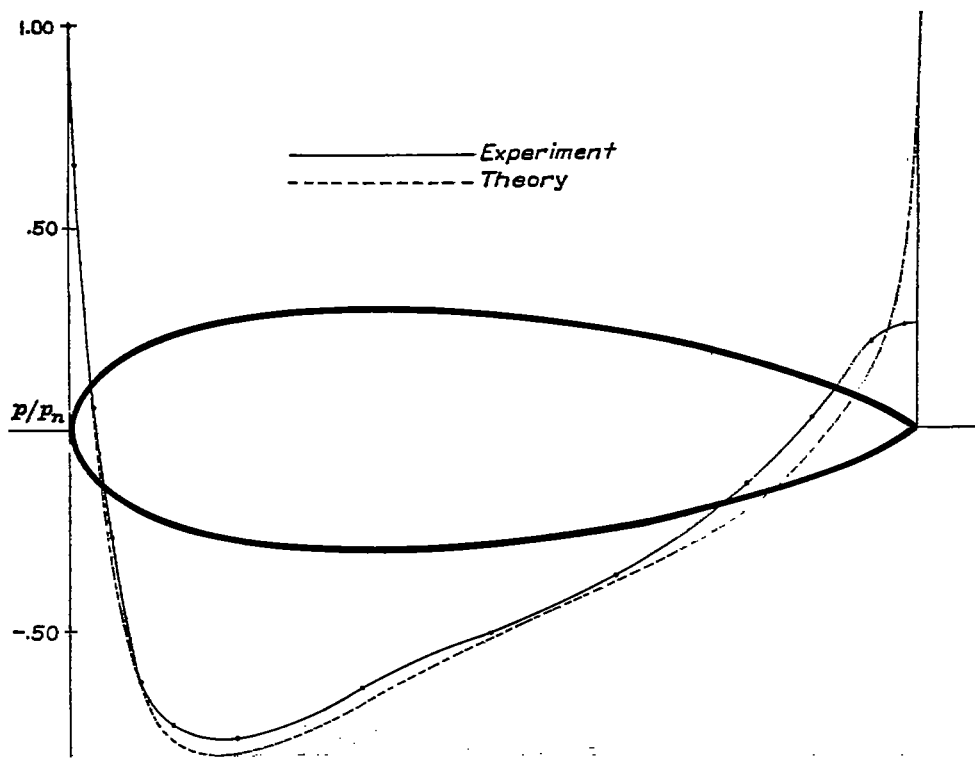
FIGURE 30.—Experimental and theoretical point pressure, p/p_n, over surface of strut No. IV
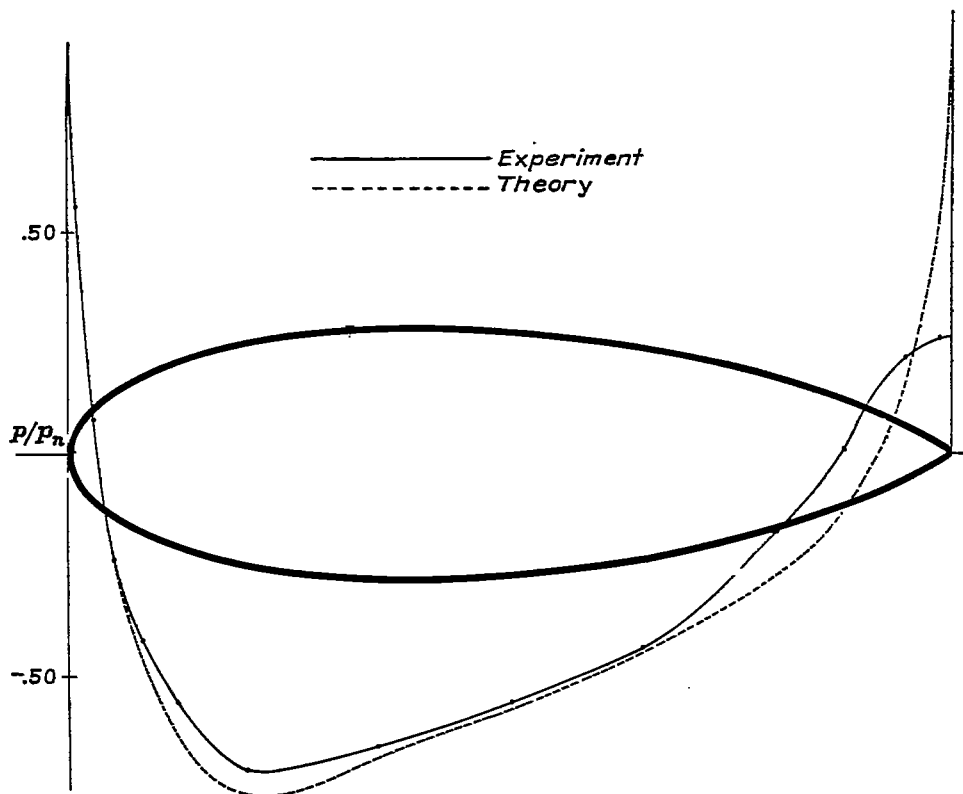
FIGURE 31.—Experimental and theoretical point pressure, p/p_n, over surface of strut No. V
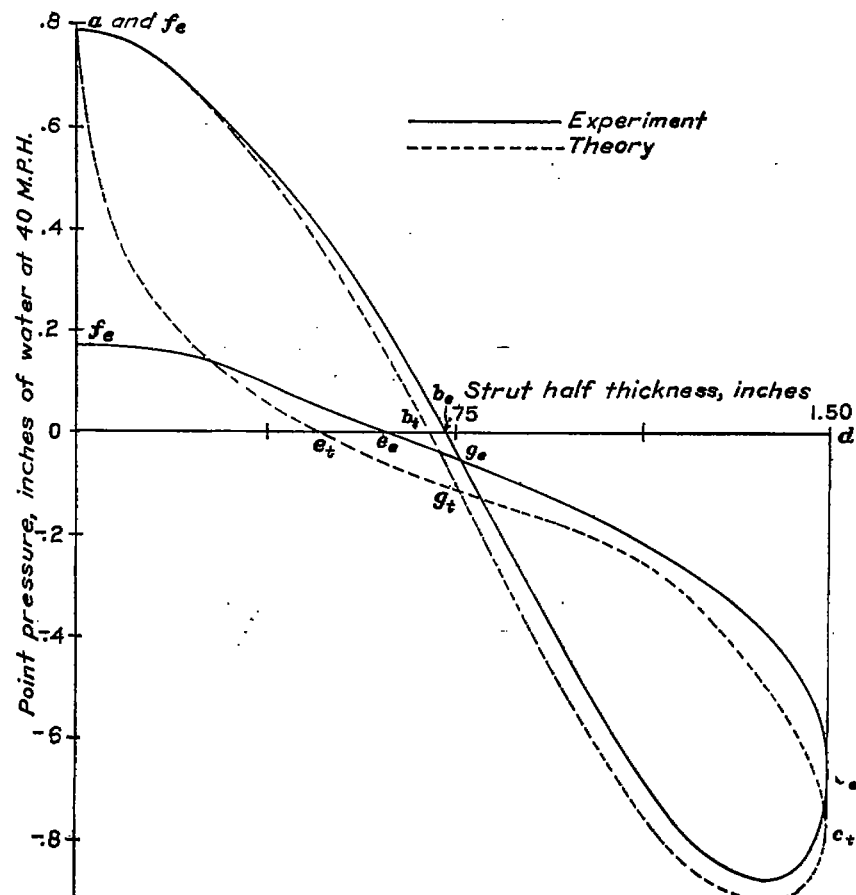
FIGURE 32.—Experimental and theoretical point pressure versus strut half thickness for strut No. I
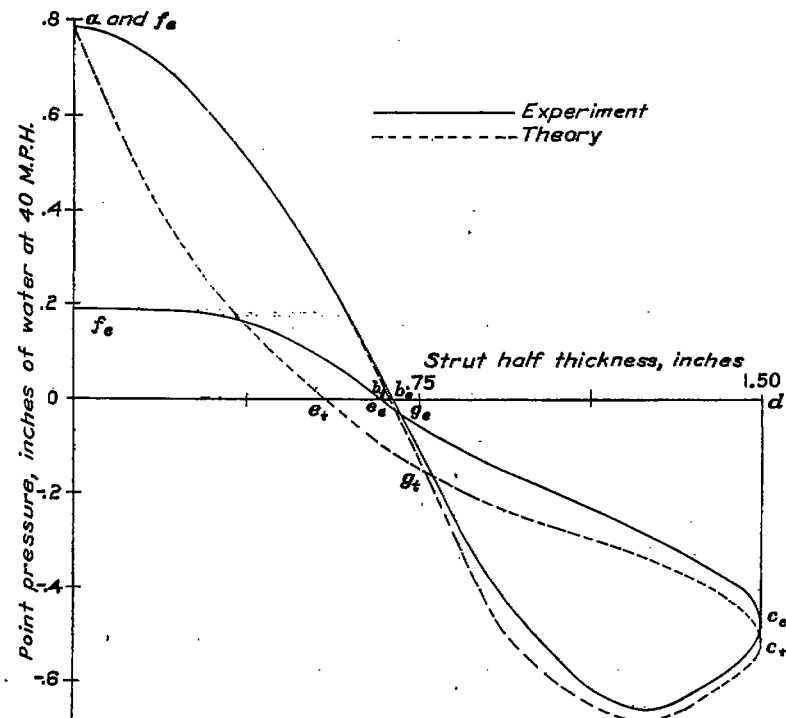
FIGURE 33.—Experimental and theoretical point pressure versus strut half thickness for strut No. II
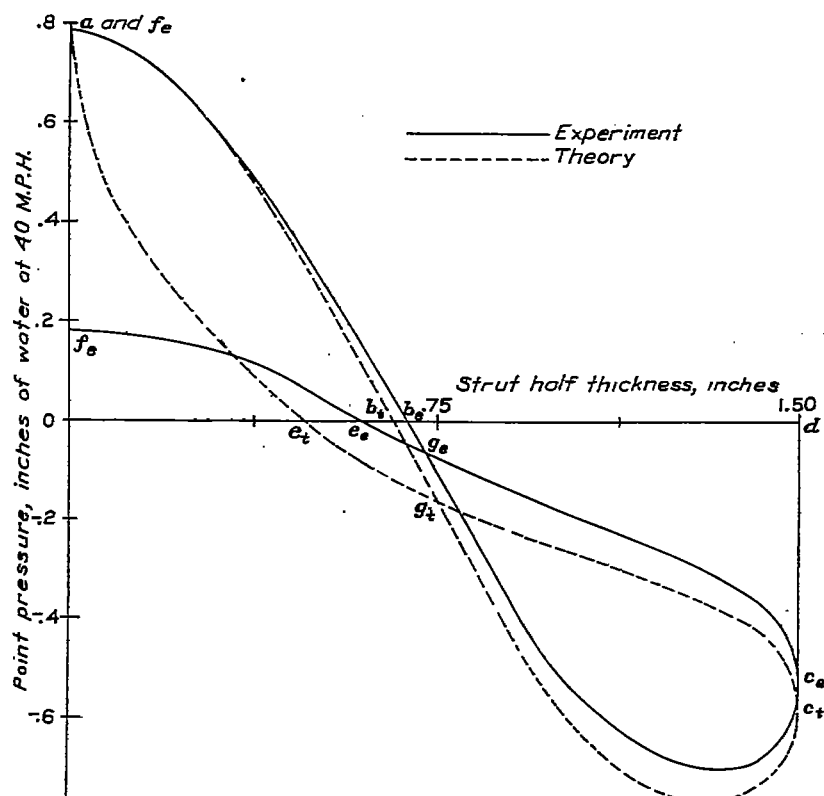
FIGURE 34.—Experimental and theoretical point pressure versus strut half thickness for strut No. III
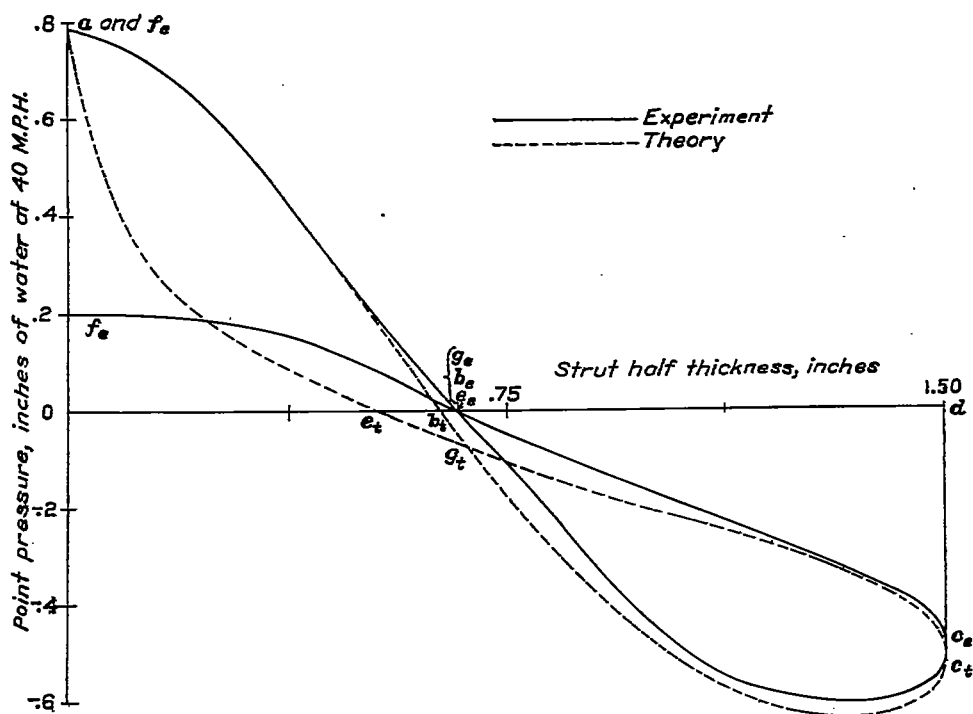
FIGURE 35.—Experimental and theoretical point pressure versus strut half thickness for strut No. IV

MODELS

The eight strut models were constructed of laminated wood and finished alike to a high polish. Strut Number I of the theoretical series of five was made of mahogany, the other four were of cherry at the bow and white pine at the stern. The three empirical struts were of white
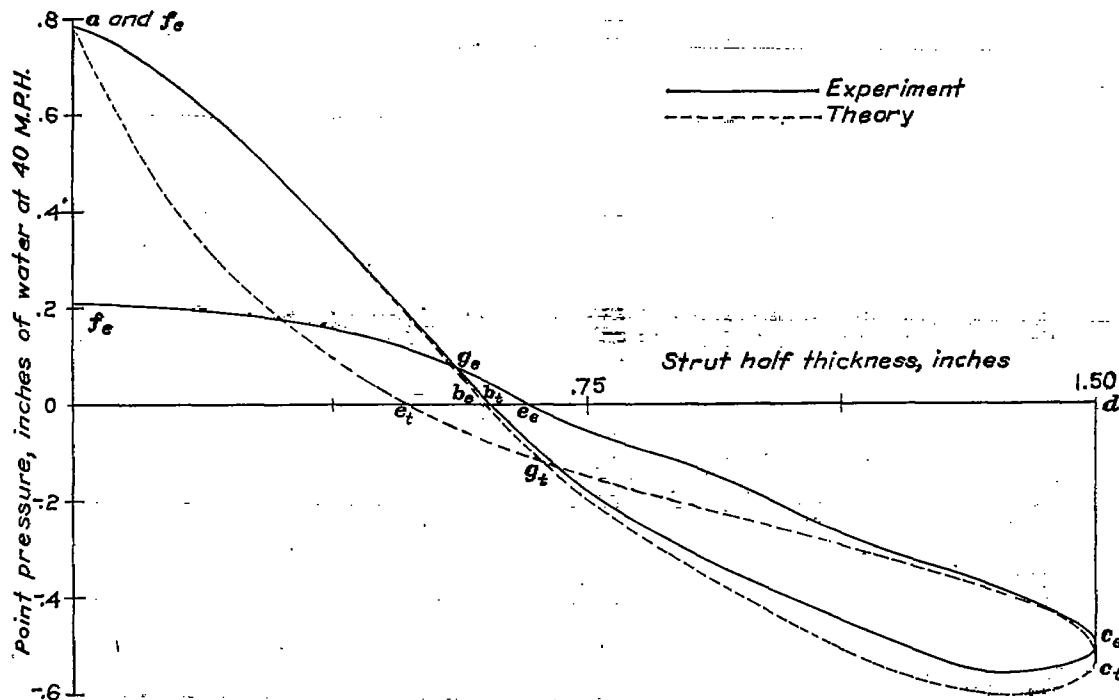
FIGURE 36.—Experimental and theoretical point pressure versus strut half thickness for strut No. V

pine only. The latter are designated R. & M. 183, being the British strut first given in R. & M. 183, but here changed from fineness-ratio 4 to 3.5 (ref. 7). Number 53 being the best German strut reported in Reference 5, and Navy Number 2 the best strut which has so far been developed in America. (Refs. 2 and 10.) All eight were 60 by 10½ by 3 inches with sections conforming to accurate metal templates made from the ordinates in Table V. Final measurements of the struts agreed with the specified ordinates everywhere well within 0.02 inch, the average error of course being much less.

FIGURE 37

At an early stage in the construction of the five theoretical struts small copper tubes were inlaid running near the surface from one end of the strut to its midsection, where they bent sharply and emerged at the surface points where pressures were to be measured. The ends of the tubes were then finished with the wood, and finally in the finished strut presented a row of pressure collectors 1 millimeter in diameter, accurately located and quite smooth. Care was taken to remove all roughness from the inner edge of the collectors. The location of the collectors is given in Tables VI to X. Figures 37 and 38, which are photographs of Strut Number V, illustrate the struts in finished form.
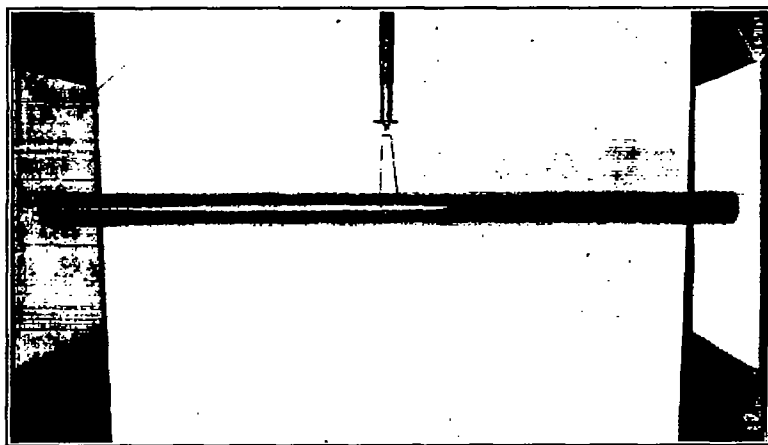
RESULTS

Table XI gives the results of the resistance tests in three froms—the resistance in pounds, the resistance coefficient based on frontal area, and the drag-strength ratio based on sectional moment of inertia. The two latter forms indicate merit of two kinds; the coefficient, C_D is a measure of merit of a strut form when its thickness is the major consideration; that is, when it is used as a fairing for round tubing or cable; the ratio D/I is a measure of merit when the strut is used in the usual way as a compression member of sufficient length to be susceptible to lateral failure as a column. Referring to Table XIa and Figure 39, Strut Number I has the greatest merit of the five as a fairing, but is poorest as a strut. Likewise Strut Number V has the greatest merit as a strut, but is only second best as a fairing. Furthermore, Table XIb and Figure 40 show that theoretical Strut Number V and the Navy Number 2 have about equal merit either as fairings or as struts and that Number 53 and R. & M. 183 follow in order of merit, the one having 3 per cent the other 12 per cent greater D/I than Number V or Navy Number 2 at R. N. 12×10^4.

The results of the pressure-distribution tests on the five theoretical struts are given in Tables VI to X in four forms: First, the point pressures referred to the bow pressure as zero are given as read in inches of alcohol along the inclined manometer tube; second, the pressures given in the first form are converted to vertical inches of water; third, those in the second form are referred to the bow pressure as $\frac{1}{2}\rho V^2$; finally, those in the third form are referred to the bow pressure as unity. The pressures in the third form are plotted along with the theoretical pressures against the strut half-thickness, y, in Figures 32 to 36 for use in integrating graphically for the four elements of pressure drag. The elements of pressure drag are listed in Table XII for both theory and experiment.
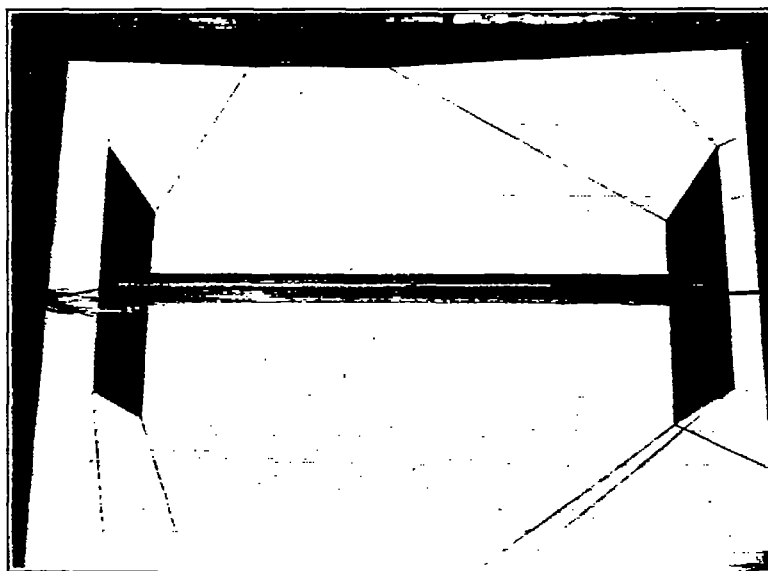
FIGURE 38

The values given show how small a residue the pressural drag is of the total upstream and the total downstream pressural forces acting and indicate the difficulty of such analyses. The table indicates that the whole drag contains from 40 to 50 per cent pressural and from 60 to 50 per cent frictional drag, when the air speed is 40 miles per hour.

The pressure coefficients, given in the fourth form in Table X, are plotted along with the theoretical pressure coefficients against the distance aft the bow in Figures 27 to 31 and show graphically the agreement between theory and experiment. In every case the experimental pressures were a little less than the theoretical over the suction range and rather uniformly so except near the stern, where the discrepancy increased and agreement became rather bad. As usual the pressures agreed near the bow and disagreed widely at the stern where the measured pressure is only one-fourth or one-fifth the theoretical value. For each strut the maximum suction occurred at the same position on the surface in both theory and experiment and moved aft and decreased in magnitude as the average strut ordinate shifted from strut to strut toward the stern.

CONCLUSIONS

Comparing Fuhrmann's results (ref. 1) with the results of this study, one finds the agreement between the theoretical and experimental pressures over the surface of low-resistance shapes rather better in three dimensional flow than in two. The consistent and uniform defi-
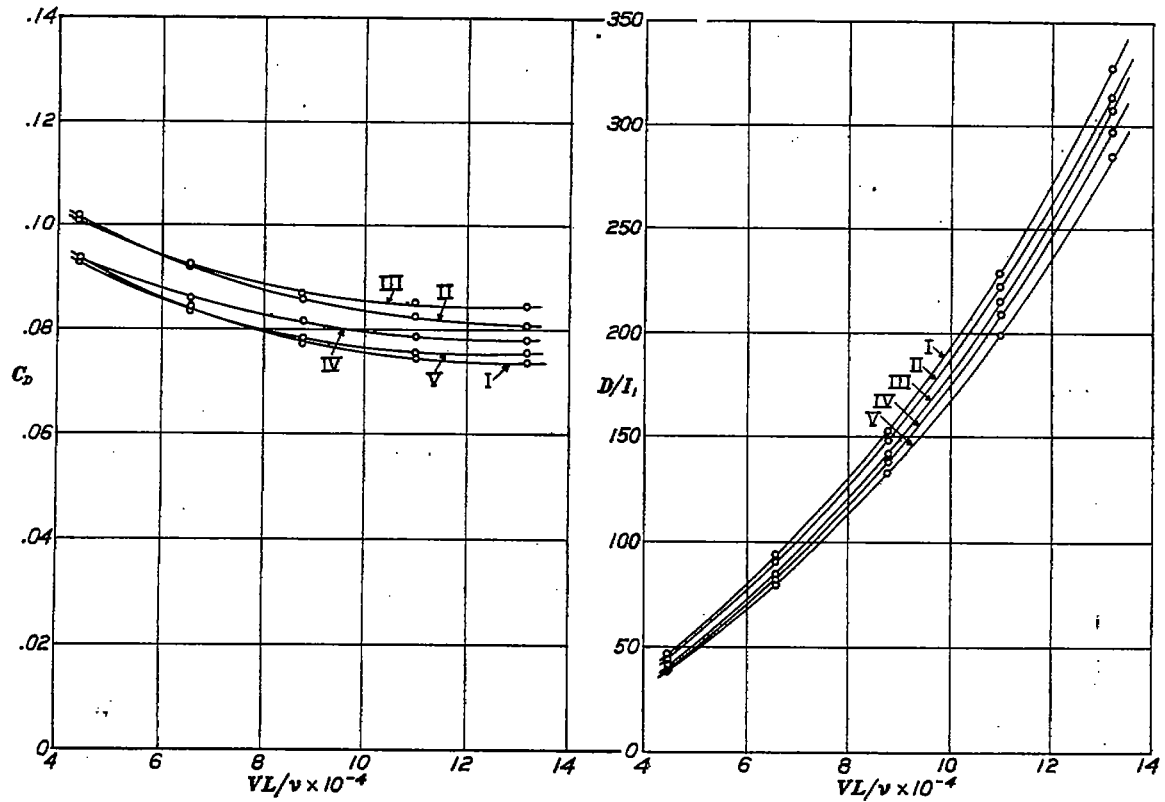
FIGURE 39
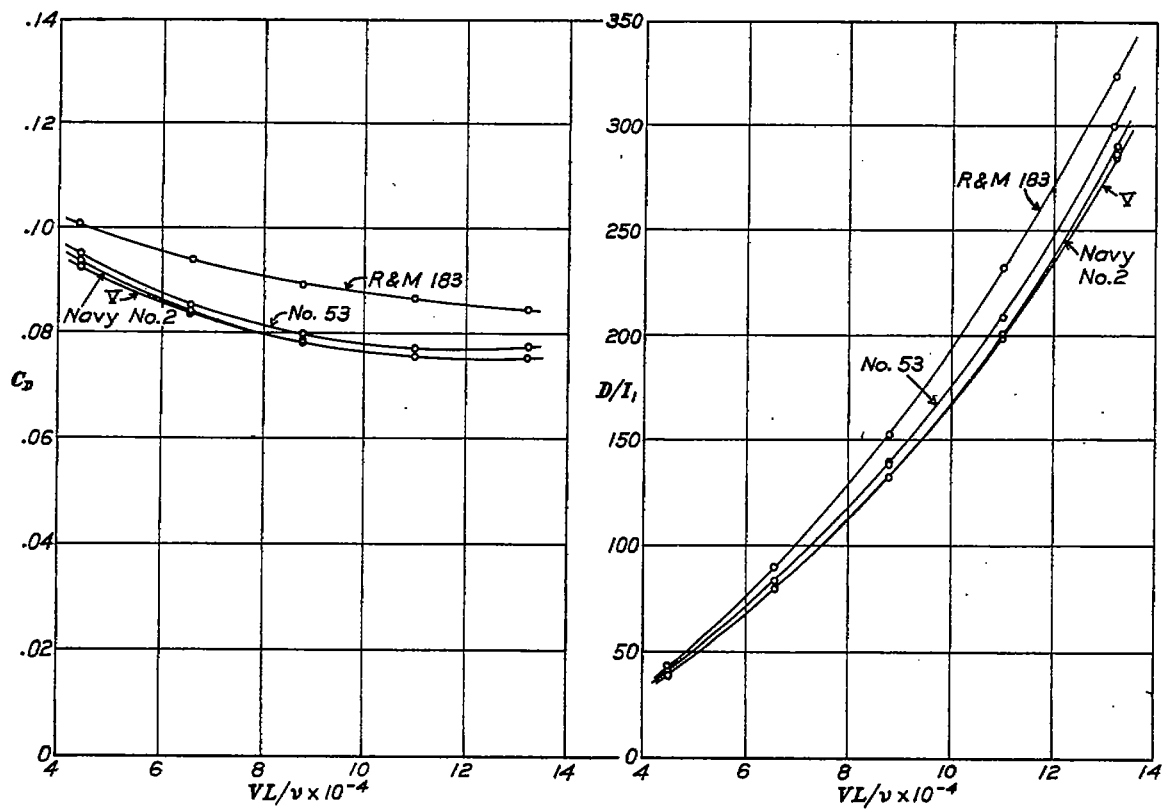
FIGURE 40

ciency of the experimental suctions found for struts does not appear in the case of Fuhrmann's airships, for which the experimental pressures were sometimes above, sometimes below, their theoretical values. While the experimental pressures at the stern agree with theory better in the case of struts than in the case of airships, the defect may be less serious for airships, from the standpoint of pressural drag, because of the relatively smaller surface area affected. Also for airships the maximum suction by experiment came at a surface position aft that by theory, while for struts the two positions are found to coincide. In case of either airships or struts the functional character of the pressure distribution is strikingly similar in theory and experiment and leaves no doubt concerning the validity of the Rankine method.

From the standpoint of practical merit, Strut Number I seems to excel as an air fairing. For column use in aircraft, Strut Number V is equally as good as the Navy Number 2 which is the best empirical air strut so far developed. These two are found by comparative test to be followed closely in merit by the German Number 53 and to be considerably better than the British R. & M. 183, the relative order of resistances being 100, 103, and 112, respectively, at 12×10^4 R. N.

It may be well to point out that these strut studies leave the air strut in a rather unique position compared to the airship. In contrasting their aerodynamic status, one finds that no theoretical airship form of high merit has been found, while a theoretical strut has been found whose merit equals that of the best empirical strut. One finds further that the theoretical flow is known about no airship of good form, excepting the approximate flow about a rigid airship form found by v. Karman (ref. 9), while the theoretical flows about the two best struts are now known and about one of these by two wholly independent methods.

REFERENCES

1. A. Fuhrmann, on "Theoretische und Experimentalle Untersuchungen an Balloonmodellen, fahrbuch der Motorluftschiff-Studien-Gesellschaft Band V.

2. A. F. Zahm, R. H. Smith, and G. C. Hill. Point Drag and Total Drag of Navy Struts No. 1 Modi-fied, Report No. 137, National Advisory Committee for Aeronautics, Washington, 1922.

3. D. W. Taylor, on Ship-Shaped Stream Forms, Transactions of the British Institution of Naval Architects, 1894.

4. A. F. Zahm, The Six-component Wind Balance, Report No. 146, National Advisory Committee for Aeronautics, Washington, 1922.

5. Max Munk. Weitere Widerstandsmessungen an Streben, Mitteilung 11 der Modell-Versuchsanstalt für Aerodynamik, Technische Berichte, Band II, 1918.

6. E. J. Gumbel, Englische Untersuchungen über den Widerstand von Streben. Technische Berichte, Band I, 1917.

7. C. H. Powell; The Resistance of Struts, Technical Report No. 416 of the Advisory Committee for Aeronautics for 1917–18.

8. A. F. Zahm; Pressure of Air on Coming to Rest from Various Speeds, Report No. 247, National Advisory Committee for Aeronautics, Washington, 1926.

9. Karman, Th. V., 1 Berechung der Druckverteilung an Luftschiffkörpern. Abhandlungen aus dem Aerodynamischen Institut an der Technischen Hochschule, Aachen. 1927.

10. Smith, R. H., Aerodynamic Theory and Test of Strut Forms, National Advisory Committee for Aeronautics, Report No. 311. Washington, 1929.

AERODYNAMICAL LABORATORY,
    BUREAU OF CONSTRUCTION AND REPAIR, U. S. NAVY,
        WASHINGTON, D. C., *April 3, 1929.*

TABLE I.—STREAM FUNCTION COEFFICIENTS, $\frac{\psi_1'}{C}$, FOR A LINE SOURCE FROM EQUATION (19)

y	x											
	0	+1.0	+2.5	+5.0	+7.5	+10.0	+20.0	+30.0	+40.0	+50.0	+60.0	+90.0
0.2	+1.5708	+0.1970	+0.0800	+0.0401	+0.0267	+0.0201	+0.0102	+0.0067	+0.0050	+0.0041	+0.0034	+0.0022
0.5	1.5708	.4362	.1970	.0998	.0666	.0500	.0250	.0167	.0125	.0102	.0083	.0056
1.0	1.5708	.7854	.3804	.1975	.1326	.0998	.0497	.0333	.0250	.0201	.0166	.0110
2.0	1.5708	1.1071	.6777	.3805	.2606	.1975	.0998	.0666	.0497	.0401	.0334	.0222
3.0	1.5708	1.2488	.8761	.5405	.3805	.2915	.1486	.0998	.0747	.0599	.0490	.0333
4.0	1.5708	1.3259	1.0123	.6778	.4898	.3805	.1946	.1326	.0998	.0800	.0666	.0444
5.3	1.5708	1.3736	1.1071	.7854	.5882	.4637	.2449	.1652	.1245	.0998	.0832	.0555
6.0	1.5708	1.4056	1.1760	.8761	.6920	.5405	.2915	.1946	.1486	.1195	.0998	.0666
7.0	1.5708	1.4288	1.2278	.9803	.7511	.6109	.3336	.2292	.1733	.1390	.1160	.0777
8.0	1.5708	1.4466	1.2680	1.0123	.8177	.6749	.3804	.2606	.1946	.1588	.1326	.0887
9.0	1.5708	1.4602	1.2997	1.0635	.8761	.7298	.4227	.2915	.2213	.1780	.1489	.0998
10.0	1.5708	1.4713	1.3258	1.1071	.9273	.7854	.4637	.3217	.2449	.1975	.1652	.1108
11.0	1.5708	1.4800	1.3473	1.1440	.9721	.8331	.5029	.3514	.2685	.2167	.1812	.1216
12.0	1.5708	1.4876	1.3654	1.1761	1.0123	.8761	.5405	.3804	.2915	.2356	.1946	.1326
13.0	1.5708	1.4940	1.3808	1.2037	1.0474	.9151	.5765	.4090	.3142	.2545	.2132	.1434
14.0	1.5708	1.4995	1.3939	1.2278	1.0789	.9503	.6109	.4366	.3366	.2731	.2292	.1542
17.0	1.5708	1.5120	1.4250	1.2850	1.1550	1.0390	.7050	.5160	.4020	.3278	.2760	.1870
20.0	1.5708	1.5210	1.4460	1.3260	1.2121	1.1071	.7850	.5880	.4640	.3805	.3220	.2190
24.0	+1.5708	+1.5290	+1.4670	+1.3650	+1.2680	+1.1760	+.8760	+.6750	+.5400	+.4477	+.3800	+.2610

TABLE II.—STREAM FUNCTION COEFFICIENTS, $\frac{\psi_1'}{C}$, FOR A SURFACE SOURCE WHOSE STRENGTH IS UNIFORMLY DISTRIBUTED FROM EQUATION (28a)

$l=10$

x	y									
	1	2	3	4	5	6	8	10	12	14
+5	0	0	0	0	0	0	0	0	0	0
+7	+0.083	+0.158	+0.222	+0.277	+0.319	+0.354	+0.405	+0.435	+0.488	+0.492
+9	.207	.369	.496	.592	.670	.734	.830	.899	.950	.989
+10	.331	.523	.666	.777	.866	.939	1.051	1.132	1.192	1.239
+11	.227	.409	.554	.667	.763	.842	.966	1.057	1.125	1.179
+13	.145	.281	.403	.510	.604	.685	.817	.920	1.002	1.065
+16	.098	.193	.286	.369	.450	.522	.651	.759	.884	.918
+20	.061	.138	.205	.269	.332	.392	.502	.601	.687	.760
+25	.051	.102	.148	.202	.250	.296	.387	.469	.548	.616
+30	.040	.081	.121	.162	.200	.239	.314	.382	.452	.515
+35	.034	.067	.101	.134	.168	.198	.262	.324	.384	.440
+40	.029	.057	.086	.115	.143	.171	.226	.280	.330	.384
+50	+.022	+.045	+.067	+.089	+.111	+.134	.178	+.220	+.263	+.303

TABLE III.—STREAM FUNCTION COEFFICIENTS, $\frac{\psi_1'}{C}$, FOR A SURFACE SOURCE WHOSE STRENGTH INCREASES LINEARLY ALONG THE WIDTH FROM EQUATION (28b)

$l=5$

x	y									
	1	2	3	4	5	6	8	10	12	14
−40	−0.0249	−0.0497	−0.0702	−0.0948	−0.1152	−0.1390	−0.1850	−0.2364	−0.2789	−0.3204
−35	−.0276	−.0525	−.0800	−.1080	−.1328	−.1576	−.2005	−.2500	−.3010	−.3492
−30	−.0286	−.0600	−.0920	−.1250	−.1582	−.1800	−.2362	−.2882	−.3400	−.3972
−25	−.0389	−.0680	−.1066	−.1379	−.1714	−.2132	−.2720	−.3407	−.3992	−.4550
−20	−.0433	−.0804	−.1288	−.2279	−.2104	−.2478	−.3310	−.4063	−.4740	−.5399
−16	−.0515	−.1025	−.1549	−.2345	−.2592	−.3030	−.3938	−.4876	−.5560	−.6288
−13	−.0597	−.1228	−.1830	−.2394	−.2986	−.3527	−.4530	−.5630	−.6404	−.7009
−10	−.0760	−.1506	−.2247	−.2938	−.3615	−.4284	−.5430	−.6659	−.7365	−.8072
−7	−.0978	−.2030	−.2866	−.3716	−.4552	−.5305	−.6632	−.7729	−.8624	−.9376
−5	−.1222	−.2355	−.3518	−.4544	−.5474	−.6228	−.7724	−.8747	−.9680	−1.0376
−2	−.1962	−.3757	−.5227	−.6397	−.7870	−.8550	−.9883	−1.0885	−1.1543	−1.2091
0	−.3425	−.5901	−.7698	−.9012	−1.0000	−1.0758	−1.1815	−1.2528	−1.3036	−1.3365
+2	−.3572	−.5631	−.6861	−.7644	−.8168	−.5841	−.9051	−.6853	−.9572	−.9728
+4	+.4000	+.2277	+.0972	+.2895	+.3155	+.3342	+.3600	+.3746	+.3896	+.3980
+5	+.7040	+.9585	+1.1088	+1.2010	+1.2640	+1.3094	+1.3701	+1.4073	+1.4352	+1.4488
+6	+.4174	+.6999	+.8838	+1.0090	+1.0986	+1.1643	+1.2580	+1.3135	+1.3528	+1.3783
+8	+.2230	+.4241	+.5906	+.7260	+.8359	+.9209	+1.0496	+1.1382	+1.2028	+1.2450
+11	+.1328	+.2606	+.3798	+.4882	+.5750	+.6723	+.8113	+.9218	+1.0084	+1.0738
+13	+.1049	+.2071	+.3050	+.4000	+.4815	+.5682	+.6945	+.8043	+.9052	+.9685
+16	+.0790	+.1568	+.2348	+.3172	+.3895	+.4475	+.5678	+.6734	+.7608	+.8356
+20	+.0610	+.1201	+.2297	+.2428	+.2997	+.2494	+.3474	+.4422	+.5425	+.6260	+.7060
+25	+.0482	+.0966	+.1390	+.1822	+.2194	+.2602	+.3471	+.4296	+.5027	+.5708
+30	+.0330	+.0769	+.0647	+.1485	+.1760	+.2096	+.2898	+.3481	+.4191	+.4837
+35	+.0306	+.0679	+.0900	+.1212	+.1577	+.1787	+.2438	+.3011	+.3606	+.4228
+40	+.0283	+.0561	+.0796	+.1313	+.1293	+.1565	+.2174	+.2628	+.3178	+.3751
+50	+.0202	+.0404	+.0618	+.0840	+.1050	+.1254	+.1657	+.2172	+.2569	+.2966

TABLE III.—STEAM FUNCTION COEFFICIENTS, $\frac{\psi_1'}{C}$, FOR A SURFACE SOURCE WHOSE STRENGTH INCREASES LINEARLY ALONG THE WIDTH FROM EQUATION (28b)—Con.

$l=20$

x	y									
	1	2	3	4	5	6	8	10	12	14
−40	−0.0189	−0.0380	−0.0588	−0.0747	−0.0943	−0.1120	−0.1497	−0.1867	−0.2209	−0.2591
−35	−.0210	−.0420	−.0626	−.0856	−.1051	−.1241	−.1654	−.2055	−.2443	−.2844
−30	−.0233	−.0470	−.0699	−.0909	−.1165	−.1379	−.1835	−.2294	−.2691	−.3181
−25	−.0267	−.0508	−.0796	−.1055	−.1315	−.1574	−.2141	−.2588	−.3076	−.3556
−20	−.0307	−.0610	−.0913	−.1231	−.1520	−.1817	−.2404	−.2961	−.3519	−.4042
−16	−.0351	−.0700	−.1049	−.1395	−.1731	−.2075	−.2732	−.3365	−.4251	−.4544
−13	−.0394	−.0783	−.1177	−.1562	−.1981	−.2318	−.2505	−.3701	−.4375	−.5001
−10	−.0451	−.0899	−.1341	−.1780	−.2209	−.2630	−.3436	−.4194	−.4899	−.5552
−7	−.0529	−.1029	−.1565	−.2065	−.2562	−.3089	−.3941	−.4772	−.5529	−.6219
−5	−.0597	−.1185	−.1765	−.2327	−.2871	−.3393	−.4363	−.5245	−.6036	−.6744
−2	−.0757	−.1495	−.2204	−.2857	−.3512	−.4107	−.5188	−.6133	−.6952	−.7672
0	−.0962	−.1849	−.2669	−.3425	−.4122	−.4764	−.5901	−.6869	−.7696	−.8408
+2	−.1146	−.2164	−.3074	−.3894	−.4635	−.5305	−.6468	−.7431	−.8240	−.8916
+4	−.1199	−.2261	−.3195	−.4024	−.4759	−.5413	−.6514	−.7400	−.8114	−.8700
+5	−.1141	−.1886	−.3017	−.3791	−.4458	−.5055	−.5911	−.6796	−.7406	−.7898
+6	−.0924	−.1712	−.2383	−.2950	−.3435	−.3843	−.4756	−.5000	−.5377	−.5574
+8	−.0522	−.0922	−.1222	−.1444	−.1619	−.1749	−.1748	−.1791	−.2109	−.2177
+11	+.0426	+.0603	+.0724	+.1009	+.1269	+.1522	+.1819	+.2165	+.2433	+.2726
+13	+.1013	+.1972	+.2798	+.3494	+.4080	+.4446	+.5336	+.5974	+.6514	+.6812
+16	+.3035	+.4755	+.6033	+.6960	−.7860	+.8548	+.9633	+1.0451	+1.1087	+1.1596
+20	+.1602	+.3040	+.4266	+.5304	+.6241	+.6914	+.8180	+.9186	+.9981	+1.0504
+25	+.1008	+.2046	+.2889	+.3763	+.4543	+.5259	+.6573	+.7519	+.8363	+.9065
+30	+.0647	+.1290	+.1884	+.2522	+.3430	+.3668	+.4718	+.5643	+.6424	+.7207
+35	+.0483	+.0967	+.1435	+.1901	+.2369	+.2809	+.3666	+.4462	+.5230	+.5879
+40	+.0357	+.0774	+.0884	+.1482	+.1896	+.2264	+.2985	+.3421	+.4308	+.4939
+50	+.0277	+.0549	+.0837	+.1116	+.1361	+.1650	+.2170	+.2709	+.3208	+.3681

TABLE IV.—STREAM FUNCTION COEFFICIENTS, $\frac{\psi_1'}{C}$, FOR A SURFACE SOURCE WHOSE STRENGTH INCREASES PARABOLICALLY ALONG THE WIDTH, FROM EQUATION (28c)

$l=10$

x	y									
	1	2	3	4	5	6	8	10	12	14
−40	−0.020	−0.060	−0.060	−0.080	−0.101	−0.121	−0.162	−0.205	−0.250	−0.288
−35	−.021	−.042	−.066	−.092	−.118	−.142	−.190	−.239	−.281	−.320
−30	−.024	−.048	−.080	−.112	−.138	−.160	−.219	−.268	−.315	−.356
−25	−.030	−.062	−.095	−.132	−.158	−.188	−.252	−.310	−.358	−.407
−20	−.037	−.072	−.115	−.155	−.187	−.221	−.292	−.360	−.420	−.475
−16	−.046	−.090	−.140	−.180	−.218	−.255	−.337	−.413	−.482	−.540
−13	−.052	−.102	−.150	−.200	−.245	−.288	−.386	−.468	−.545	−.602
−10	−.060	−.119	−.177	−.230	−.279	−.327	−.436	−.536	−.611	−.679
−7	−.070	−.143	−.211	−.272	−.333	−.392	−.505	−.622	−.708	−.769
−5	−.083	−.163	−.238	−.311	−.379	−.449	−.568	−.690	−.780	−.844
−2	−.111	−.216	−.316	−.404	−.479	−.566	−.702	−.817	−.909	−.976
0	−.150	−.284	−.409	−.505	−.594	−.683	−.825	−.932	−1.022	−1.084
+2	−.217	−.381	−.527	−.643	−.744	−.826	−.953	−1.060	−1.129	−1.177
+5	−.258	−.416	−.555	−.647	−.710	−.767	−.837	−.900	−.947	−.977
+7	−.192	−.280	−.353	−.383	−.398	−.414	−.446	−.473	−.487	−.500
+9	+.154	+.218	+.310	+.399	+.467	+.480	+.535	+.581	+.632	+.662
+10	+.580	+.832	+.975	+1.076	+1.151	+1.213	+1.298	+1.336	+1.368	+1.401
+11	+.351	+.605	+.772	+.909	+.990	+1.056	+1.183	+1.243	+1.288	+1.320
+13	+.204	+.375	+.525	+.650	+.738	+.822	+.988	+1.076	+1.130	+1.186
+16	+.122	+.242	+.340	+.437	+.520	+.601	+.756	+.863	+.949	+1.021
+20	+.082	+.154	+.233	+.313	+.370	+.446	+.577	+.678	+.770	+.843
+25	+.063	+.118	+.170	+.228	+.273	+.325	+.432	+.525	+.608	+.668
+30	+.045	+.088	+.132	+.175	+.217	+.262	+.340	+.420	+.490	+.555
+35	+.036	+.072	+.109	+.142	+.178	+.219	+.279	+.352	+.413	+.475
+40	+.030	+.060	+.089	+.120	+.151	+.182	+.243	+.299	+.353	+.415
+50	+.023	+.046	+.069	+.092	+.115	+.137	+.182	+.230	+.304	+.320

TABLE Va.—ORDINATES GIVING THE SURFACES OF THE FIVE RANKINE STRUTS

Strut No. I		Strut No. II		Strut No. III		Strut No. IV		Strut No. V	
x	y	x	y	x	y	x	y	x	y
0	0	0	0	0	0	0	0	0	0
0.049	0.304	0.053	0.294	0.049	0.270	0.053	0.233	0.017	0.131
.098	.441	.152	.500	.098	.402	.217	.520	.052	.248
.196	.618	.250	.642	.196	.564	.422	.726	.086	.316
.294	.750	.348	.755	.294	.699	.627	.882	.189	.454
.392	.848	.495	.892	.441	.833	.832	.996	.292	.564
.539	.980	.642	.995	.588	.936	1.037	1.094	.430	.678
.686	1.080	.887	1.127	.833	1.073	1.446	1.283	.602	.791
.931	1.211	1.132	1.230	1.078	1.176	1.856	1.332	.774	.884
1.176	1.302	1.377	1.309	1.323	1.250	2.266	1.406	.946	.970
1.421	1.368	1.622	1.363	1.569	1.304	2.676	1.451	1.118	1.042
1.667	1.417	2.113	1.436	2.059	1.397	3.086	1.483	1.462	1.170
2.157	1.477	2.603	1.475	2.549	1.451	3.495	1.500	1.806	1.272
2.647	1.500	3.093	1.497	3.039	1.485	3.905	1.496	2.150	1.342
3.137	1.490	3.583	1.500	3.529	1.496	4.315	1.487	2.494	1.397
3.627	1.456	4.073	1.484	4.017	1.500	5.135	1.436	2.838	1.435
4.118	1.408	4.564	1.451	4.510	1.490	5.954	1.352	3.526	1.486
4.608	1.348	5.054	1.402	5.000	1.466	6.774	1.229	4.214	1.500
5.588	1.196	5.544	1.348	5.490	1.421	7.593	1.065	4.902	1.476
6.569	1.010	6.524	1.196	6.471	1.294	8.413	.861	5.500	1.428
7.549	.799	7.505	1.010	7.451	1.118	8.823	.746	6.278	1.352
8.529	.569	8.485	.770	8.431	.882	9.233	.615	6.967	1.249
9.020	.441	8.975	.627	8.922	.745	9.642	.467	7.655	1.101
9.510	.318	9.466	.470	9.412	.578	10.052	.287	8.343	.925
10.000	.186	9.711	.382	9.902	.387	10.257	.180	9.031	.712
10.245	.122	9.956	.284	10.147	.274	10.462	.061	9.375	.598
10.490	.029	10.201	.176	10.385	.147	10.519	0	9.719	.460
10.519	0	10.446	.056	10.455	.083			10.063	.275
		10.505	0	10.519	0			10.235	.186
								10.407	.072
								10.486	0

TABLE Vb.—ORDINATES GIVING THE SURFACES OF THE R. & M. 183 (BRITISH), NO. 53 (GERMAN), AND NAVY No. 2 (AMERICAN) STRUTS

R. & M. 183		No. 53		Navy No. 2	
x	y	x	y	x	y
0	0	0	0	0	0
0.210	0.345	0.054	0.237	0.262	0.555
.525	.720	.189	.481	.525	.792
.788	.936	.378	.680	.787	.952
1.050	1.092	.607	.846	1.050	1.080
1.575	1.306	.905	1.022	1.312	1.180
2.100	1.440	1.215	1.164	1.575	1.260
2.625	1.487	1.592	1.298	1.837	1.320
3.150	1.500	2.119	1.418	2.100	1.375
3.675	1.495	2.632	1.477	2.625	1.440
4.200	1.475	3.361	1.500	3.150	1.480
4.725	1.443	4.192	1.498	3.675	1.500
5.250	1.404	4.860	1.457	4.200	1.500
5.775	1.344	5.540	1.380	4.725	1.498
6.300	1.272	6.273	1.275	5.250	1.440
6.825	1.187	6.900	1.151	5.775	1.378
7.350	1.092	7.588	1.004	6.300	1.290
7.875	.979	8.330	.810	6.825	1.207
8.400	.852	8.975	.620	7.350	1.107
8.925	.711	9.592	.413	7.875	.983
9.450	.564	10.000	.250	8.400	.852
9.975	.376	10.302	.102	8.925	.698
10.340	.186	10.500	0	9.450	.510
10.500	0			9.975	.292
				10.500	0

TABLE VI.—THEORETICAL AND EXPERIMENTAL VELOCITIES AND PRESSURES ON THE SURFACE OF STRUT No. I AT 40 MILES PER HOUR

Hole No.	Hole position		Theoretical			Experimental				
	x	y	Velocity	Pressure p	p/p_a	[1]	[2]	p	p/p_a	Velocity
1	0	0	0	+0.787	+1.000	0	0	+0.787	+1.000	0
2	0.100	0.446	27.9	+.412	+.516	4.08	−.323	+.464	+.589	25.7
3	.300	.766	43.8	−.157	−.200	−10.89	−.857	−.030	−.038	40.8
4	.550	.997	52.1	−.546	−.694	−15.97	−1.261	−.474	−.602	50.7
5	.880	1.192	57.3	−.828	−1.053	−19.86	−1.567	−.780	−.991	56.5
6	1.300	1.348	58.9	−.913	−1.160	−21.10	−1.665	−.878	−1.117	58.2
7	2.100	1.472	57.8	−.853	−1.084	−20.00	−1.578	−.791	−1.005	56.7
8	3.640	1.461	53.8	−.635	−.807	−16.55	−1.314	−.527	−.669	51.7
9	5.240	1.255	48.3	−.358	−.455	−13.70	−1.081	−.294	−.374	46.9
10	6.800	.962	44.4	−.183	−.233	−11.75	−.927	−.140	−.178	43.4
11	8.400	.599	41.4	−.057	−.072	−9.91	−.781	+.006	+.008	39.8
12	9.220	.383	39.1	+.036	+.046	−8.95	−.706	+.081	+.103	37.9
13	9.950	.206	34.8	+.191	+.243	−7.98	−.629	+.158	+.201	35.8
14	10.350	.083	31.4	+.393	+.500	−7.81	−.616	+.171	+.218	35.4

[1] Inches of alcohol 1 to 10.   [2] Inches of water vertical.

TABLE VII.—THEORETICAL AND EXPERIMENTAL VELOCITIES AND PRESSURES ON THE SURFACE OF STRUT No. II AT 40 MILES PER HOUR

Hole No.	Hole position		Theoretical			Experimental				Velocity
				Pressure		Pressure				
	x	y	Velocity	p	p/p_n	(1)	(2)	p	p/p_n	
1	0	0	0	+0.787	+1.000	0	0	+0.787	+1.000	0
2	.100	0.432	26.4	+.443	+.563	-4.32	-.342	+.446	+.566	26.4
3	.300	.712	41.1	-.045	-.058	-10.55	-.831	-.044	-.056	41.1
4	.550	.933	50.5	-.465	-.592	-15.71	-1.239	-.452	-.575	50.2
5	.880	1.118	55.0	-.702	-.892	-17.81	-1.406	-.619	-.789	53.5
6	1.300	1.275	56.3	-.769	-.978	-18.79	-1.483	-.696	-.885	54.9
7	2.100	1.422	55.3	-.716	-.910	-18.36	-1.449	-.662	-.842	54.3
8	3.640	1.496	52.1	-.546	-.694	-16.19	-1.273	-.491	-.623	51.0
9	5.240	1.393	49.3	-.410	-.521	-14.45	-1.141	-.354	-.450	48.2
10	6.800	1.152	47.3	-.311	-.395	-12.96	-1.023	-.236	-.300	45.6
11	8.400	.800	44.3	-.178	-.227	-11.16	-.881	-.094	-.120	42.3
12	9.220	.564	41.4	-.065	-.070	-9.67	-.763	+.024	+.031	39.4
13	9.950	.309	35.7	+.157	+.200	-8.17	-.645	+.142	+.180	36.2
14	10.350	.108	27.4	+.418	+.532	-7.06	-.557	+.230	+.280	35.1

¹ Inches of alcohol 1 to 10.   ² Inches of water vertical.

TABLE VIII.—THEORETICAL AND EXPERIMENTAL VELOCITIES AND PRESSURES ON THE SURFACE OF STRUT No. III AT 40 MILES PER HOUR

Hole No.	Hole position		Theoretical			Experimental				Velocity
				Pressure		Pressure				
	x	y	Velocity	p	p/p_n	(1)	(2)	p	p/p_n	
1	0	0	0	+0.787	+1.000	0	0	+0.787	+1.000	0
2	0.100	0.407	23.3	+.519	+.660	-3.28	-.258	+.529	+.672	22.9
3	.300	.711	42.7	-.110	-.140	-11.30	-.892	-.105	-.133	42.6
4	.550	.913	50.6	-.472	-.600	-15.10	-1.192	-.405	-.574	49.3
5	.880	1.108	54.1	-.650	-.826	-17.90	-1.413	-.626	-.796	53.6
6	1.300	1.240	54.8	-.686	-.872	-18.34	-1.447	-.660	-.839	54.3
7	2.100	1.393	53.4	-.614	-.781	-17.36	-1.368	-.581	-.739	52.8
8	3.640	1.500	51.3	-.506	-.643	-16.09	-1.267	-.450	-.610	50.7
9	5.240	1.437	49.8	-.431	-.548	-15.20	-1.200	-.413	-.525	49.4
10	6.800	1.230	47.9	-.341	-.434	-13.85	-1.091	-.304	-.386	47.1
11	8.400	.893	45.0	-.209	-.266	-11.43	-.902	-.211	-.166	43.2
12	9.220	.653	42.1	-.083	-.106	-9.77	-.770	+.017	+.022	39.6
13	9.950	.427	37.4	+.099	+.126	-8.02	-.632	+.155	+.197	35.8
14	10.350	.172	26.8	+.433	+.551	-7.58	-.598	+.189	+.240	34.9

¹ Inches of alcohol 1 to 10.   ² Inches of water vertical.

TABLE IX.—THEORETICAL AND EXPERIMENTAL VELOCITIES AND PRESSURES ON THE SURFACE OF STRUT No. IV AT 40 MILES PER HOUR

Hole No.	Hole position		Theoretical			Experimental				Velocity
				Pressure		Pressure				
	x	y	Velocity	p	p/p_n	(1)	(2)	p	p/p_n	
1	0	0	0	+0.787	+1.000	0	0	+0.787	+1.000	0
2	.100	.323	23.6	+.514	+.653	-3.39	-0.268	+.519	+.659	23.4
3	.300	.606	39.0	+.039	+.050	-9.44	-.745	+.042	+.053	38.9
4	.550	.819	45.4	-.289	-.368	-12.64	-.998	-.211	-.268	45.1
5	.880	1.023	51.3	-.503	-.640	-16.32	-1.288	-.501	-.637	51.2
6	1.300	1.183	53.3	-.609	-.774	-17.38	-1.370	-.583	-.741	52.8
7	2.100	1.375	53.8	-.636	-.808	-17.72	-1.399	-.612	-.778	53.4
8	3.640	1.486	53.4	-.616	-.783	-16.46	-1.299	-.512	-.650	51.4
9	5.240	1.433	49.3	-.408	-.518	-15.03	-1.185	-.398	-.506	49.1
10	6.800	1.228	47.0	-.298	-.379	-13.60	-1.073	-.286	-.363	46.7
11	8.400	.863	44.0	-.163	-.208	-11.32	-.893	-.106	-.135	42.6
12	9.220	.623	41.2	-.047	-.060	-9.70	-.766	+.021	+.027	39.5
13	9.950	.336	37.0	+.115	+.147	-7.88	-.620	+.167	+.212	35.5
14	10.350	.128	32.7	+.334	+.425	-7.44	-.587	+.200	+.254	34.5

¹ Inches of alcohol 1 to 10.   ² Inches of water vertical.

TABLE X.—THEORETICAL AND EXPERIMENTAL VELOCITIES AND PRESSURES ON THE SURFACE OF STRUT No. V AT 40 MILES PER HOUR

Hole No.	Hole position		Theoretical			Experimental				Velocity
	x	y	Velocity	Pressure		Pressure				
				p	p/p_n	(1)	(2)	p	p/p_n	
1	0	0	0	+0.787	+1.000	0	0	+0.787	+1.000	0
2	.100	.328	26.7	+.487	+.556	−4.42	−0.349	+.438	+.556	26.7
3	.300	.579	38.5	+.057	+.073	−9.22	−.727	+.060	+.076	38.5
4	.550	.717	44.7	−.194	−.247	−12.36	−.976	−.189	−.240	44.6
5	.880	.941	48.4	−.366	−.465	−12.90	−1.019	−.332	−.422	47.7
6	1.300	1.112	51.2	−.504	−.640	−15.55	−1.227	−.440	−.559	49.9
7	2.100	1.336	53.2	−.606	−.770	−17.14	−1.353	−.566	−.719	52.5
8	3.640	1.498	52.0	−.542	−.689	−16.60	−1.310	−.523	−.665	51.6
9	5.240	1.452	50.2	−.456	−.579	−15.59	−1.230	−.443	−.563	50.0
10	6.800	1.263	48.2	−.356	−.452	−14.40	−1.136	−.349	−.443	48.1
11	8.400	.913	45.1	−.215	−.273	−11.73	−.926	−.139	−.177	43.4
12	9.220	.648	42.5	−.100	−.127	−9.99	−.785	+.002	+.003	39.9
13	9.950	.352	37.4	+.123	+.156	−7.85	−.620	+.167	+.212	35.5
14	10.350	.138	30.1	+.434	+.552	−7.40	−.584	+.203	+.258	34.5

¹ Inches of alcohol, 1 to 10.   ² Inches of water vertical.

TABLE XIa.—RESISTANCE VALUES PER FOOT RUN FOR FIVE RANKINE STRUTS AT VARIOUS AIR SPEEDS AND ZERO PITCH AND YAW

Air speed V in miles per hour	Strut					$\frac{V_1 L_1}{(ft)^2}$ sec	$\frac{V_1 L_1}{\nu}$ ×10⁻⁴
	I	II	III	IV	V		
Drag, D, in pounds per foot run							
20	0.0240	0.0260	0.0258	0.0240	0.0238	7.34	4.40
30	.0486	.0532	.0534	.0494	.0472	11.00	6.59
40	.0788	.0876	.0888	.0834	.0801	14.67	8.79
50	.1190	.1320	.1362	.1260	.1204	18.34	10.98
60	.1700	.1858	.1940	.1792	.1740	22.00	13.18
Drag coefficient $C_D = \frac{2Dg}{\rho A V_1^2}$							
20	.0940	.1018	.1010	.0940	.0931	7.34	4.40
30	.0845	.0926	.0929	.0859	.0821	11.00	6.59
40	.0772	.0858	.0870	.0817	.0784	14.67	8.79
50	.0745	.0826	.0854	.0789	.0753	18.34	10.98
60	.0739	.0808	.0844	.0780	.0758	22.00	13.18
Drag-strength ratio, $\frac{D}{I_1}$, $\frac{lb./foot}{(feet)^4}$							
20	46.23	43.78	40.91	39.86	39.09	7.34	4.40
30	93.62	89.59	84.67	82.04	77.53	11.00	6.59
40	151.80	147.51	140.80	138.50	131.57	14.67	8.79
50	229.24	222.28	215.95	209.26	197.77	18.34	10.98
60	327.49	312.88	307.60	297.60	285.81	22.00	13.18
Sectional moment of inertia I, in.⁴							
	10.764	12.314	13.078	12.486	12.624		

L_1=strut thickness in feet =⅓.
A=frontal area of strut in ft.²/ft.=⅓.
V_1=air speed in feet per second.
ρ/g=0.00237 slug. ν=0.0001670 (ft.)²/sec.
I_1=moment of inertia in ft.⁴

TABLE XIb.—RESISTANCE VALUES PER FOOT RUN FOR RANKINE STRUT NO. V COMPARED WITH THOSE FOR R. & M. 183 (BRITISH), No. 53 (GERMAN), NAVY No. 2 (AMERICAN)

Air speed V in miles per hour	Strut				$V_1 L_1$ (ft.)^2 sec.	$\dfrac{V_1 L_1}{\nu}$ $\times 10^{-4}$
	R. & M. 183	No. 53	Navy 2	V		
	Drag, D, in pounds per foot run					
20	0. 0258	0. 0243	0. 0240	0. 0238	7. 34	4. 40
30	. 0544	. 0484	. 0472	. 0472	11. 00	6. 59
40	. 0912	. 0818	. 0796	. 0801	14. 67	8. 79
50	. 1390	. 1230	. 1206	. 1204	18. 34	10. 98
60	. 1938	. 1778	. 1748	. 1740	22. 00	13. 18
	Drag coefficient $C_D = \dfrac{2 Dg}{\rho A V_1^2}$					
20	. 1010	. 0951	. 0940	. 0931	7. 34	4. 40
30	. 0945	. 0842	. 0821	. 0821	11. 00	6. 59
40	. 0893	. 0800	. 0779	. 0784	14. 67	8. 79
50	. 0870	. 0769	. 0755	. 0753	18. 34	10. 98
60	. 0844	. 0774	. 0761	. 0758	22. 00	13. 18
	Drag-strength ratio, $\dfrac{D}{I_1}$, $\dfrac{\text{lb./foot}}{(\text{feet})^4}$					
20	43. 09	40. 99	39. 90	39. 09	7. 34	4. 40
30	90. 85	81. 65	78. 46	77. 53	11. 00	6. 59
40	152. 31	137. 99	132. 32	131. 57	14. 67	8. 79
50	232. 15	207. 50	200. 48	197. 77	18. 34	10. 98
60	323. 67	299. 94	290. 58	285. 81	22. 00	13. 18
	Sectional moment of inertia I in.^{4}					
	12. 416	12. 292	12. 474	12. 624		

TABLE XII.—ALONG STREAM FORCES PER FOOT RUN OF STRUTS IN 40 MILES PER HOUR AIR SPEED

	Strut No.	Downstream			Upstream			Pressural drag $D_p = P_1 - p^1$	Frictional drag D_f	Total drag $D = D_p + D_f$
		Push	Suction	Total p_1	Push	Suction	Total p_2			
Theoretical		Pounds per foot run								
	I	0. 298	0. 214	0. 512	0. 086	0. 426	0. 512	0	0	0
	II	. 281	. 223	. 504	. 110	. 396	. 506	−. 002	0	0
	III	. 291	. 209	. 500	. 146	. 358	. 504	−. 004	0	0
	IV	. 256	. 181	. 437	. 099	. 338	. 437	0	0	0
	V	. 229	. 214	. 443	. 122	. 320	. 442	+. 001	0	0
Experimental		Pounds per foot run								
	I	. 313	. 164	. 477	. 056	. 382	. 438	. 039	. 040	. 079
	II	. 288	. 160	. 448	. 065	. 348	. 413	. 035	. 053	. 088
	III	. 296	. 156	. 452	. 083	. 333	. 416	. 036	. 053	. 089
	IV	. 264	. 157	. 421	. 080	. 308	. 388	. 033	. 050	. 083
	V	. 232	. 172	. 404	. 064	. 289	. 373	. 031	. 049	. 080
		Per cent of total measured drag, D								
	I	391	205	596	70	477	547	49	51	100
	II	327	182	509	74	395	469	40	60	100
	III	332	175	507	93	374	467	39	61	100
	IV	318	189	507	96	371	467	40	60	100
	V	290	215	505	105	361	466	39	61	100